Examples of microstructures in metallic materials

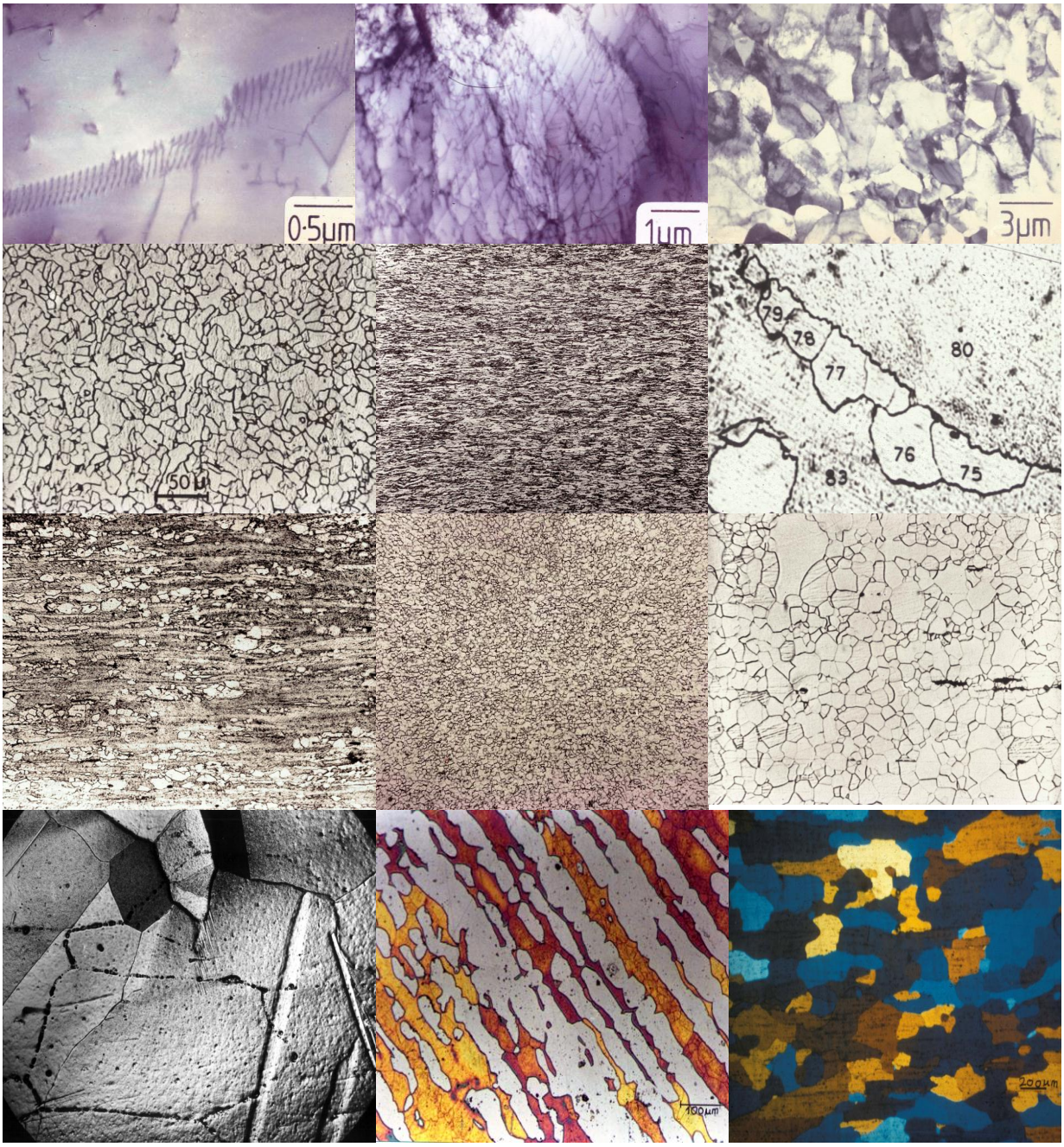

C. Dasarathy **February 2012**

Table of contents

Section	Contents	Page number
1	Introduction	4
2	The background to the importance of microstructures in materials	4
3	Microstructures in steels	8
3.1	Continuous casting	8
3.2	Hot rolling to sheet/strip	11
3.3	Precipitation during hot rolling	13
3.4	Cooling after completion of hot rolling leads to phase transformation	13
3.5	Precipitation observed in hot rolled steels	16
3.6	Microstructures of sheet steels after cold rolling and annealing	21
3.6.1	Microstructures and other features of the cold rolled steel	21
3.6.2	Annealing heat treatments of the cold rolled strip	22
3.6.3	Precipitation during batch annealing of aluminium stabilised steels	26
3.6.4	The role of precipitates in the secondary recrystallisation of steels	28
3.6.5	Carbon precipitation on dislocations	31
3.7	Martensitic steels	32
3.8	Austenitic and duplex stainless steels	33
4	Deformation, recrystallisation and grainboundary migration in materials other than steels	35
4.1	Very dilute alloys of indium with iron	35
4.2	Electron beam irradiation of thin foils of indium	36

4.3	Grainboundary migration in indium deformed at a sub-zero temperature	37
4.4	Is there a phase transformation in indium ?	40
4.5	The deformation and recrystallisation behaviour of bismuth	40
4.6	Neumann bands in silicon steels	41
4.7	Deformation, recrystallisation in aluminium and precipitation hardening in aluminium-copper alloys	42
4.8	Copper, brasses and bronzes	48
5	Superplastic materials	52
6	Concluding remarks and acknowledgements	55
7	References	55

1. Introduction

In August 2011, I produced a compilation entitled 'Examples of fractures, failures and rejections of engineering materials and components' [1]. Over 100 examples feature in this document to illustrate how components fail in service .This compilation was done for the benefit of the students of materials sciences and engineering as well as for junior engineers and apprentices in various engineering disciplines. Amongst other websites, the document is also available as a pdf file at Wikimedia Commons; this is listed as
' **A book on failures' by Cuppam**/ Ticket Number #2011082310006175/ 25th of August 2011. This can accessed at
Wiki/File. Book on failures. PDF and at http://en.wikiversity.org.[1]

Why do components fail in service? More often than not ,this is because the properties are not up to specification. Why are the properties not up to specification ? This is essentially because the microstructures are not compatible with the properties sought after. The present compilation is undertaken to highlight the importance of microstructures of materials and is intended for the same readership as above.

Steels form a significant part of the broad spectrum of materials used in the industry. Amongst steels, sheet or strip steels form a major fraction of the steels produced. Particular attention will hence be given to this group of products in the following compilation.

2.The background to the importance of microstructures in materials

Materials are used to produce components in the industrial world. Design engineers call for specific properties in the components. Underwater jacket legs of drilling rigs used in off-shore oil installations need to withstand very low temperatures as well as the constant pounding of the waves. The materials used here must have not only high yield and tensile strengths but also have adequate impact toughness at low temperatures such as - 30 to
- 50 ^{0}C. A turbine shaft running in the high pressure section of an aircraft engine operates at high temperatures as well as at high speeds (high RPM). The materials used here must hence have high creep and fatigue strengths. Brake materials used in aircraft must provide adequate and reliable braking to bring the aircraft to a stop within a prescribed distance. Braking a commercial aircraft generates intense heat and the brakes often get red hot. The coefficient of friction must be such that despite the high temperatures the brakes get up to, the brakes provide enough friction so as to bring the aircraft to a stop. Line pipe steels that are buried underground are used in the transportation of oil and gas across Alaskan and Siberian fields where the winter temperatures plummet to very low levels. Whilst the steels may be ductile at around 20 ^{0}C, they can become very brittle at sub-zero temperatures. This points to a potential risk of the pipeline fracturing and leading to a vast spillage of oil underground. This is known as the ductile-brittle transition behaviour, typical of body centered cubic materials .The remedy lies in ensuring that the steels have adequate fracture toughness even at temperatures as low as - 50 ^{0}C. An automotive exhaust valve operates at temperatures > ~600-700 ^{0}C; the material is to have an adequate resistance to oxidation at high temperatures. A goldsmith or a silversmith needs to work with materials that have excellent ductility. These examples illustrate that the materials must be processed to give rise to these specific properties.

It must be appreciated that the properties arise as a result of the presence of specific microstructures appropriate to the requirements. Several techniques are used to examine, compare, describe and quantify the microstructures in materials. Optical microscopy, electron microscope examination of carbon extraction replicas of surfaces, transmission electron microscopy, scanning electron microscopy are examples of the tools and techniques used to study the microstructures. Several parameters are employed to describe the microstructures. These include , for example, the grain size, the ASTM number, grain shape and distribution, precipitate size, inter-particle spacing, volume fraction of precipitates, the dislocation type, density, the nature of stacking faults , etc. Based on certain empirical equations, the microstructures/properties can also be successfully predicted. The essential point to appreciate is that the development of the microstructure in a given material is central to its being used successfully in industrial application. If one were to ask the question as to which is the 'cause' and which is the 'effect', the answer would be that 'the **presence of the microstructure'** is the cause and 'the **development of the properties'** is the effect.

The above cause-effect relationship between the microstructure and the properties has a close parallel with the crystal structure of the elements and their deformation behaviour. For example, face-centered cubic (FCC) elements such as Au, Ag, Cu, Al have superior ductility because of a multiplicity of slip systems and are hence, easy to deform when cold, warm or hot. The **crystal structure** is the' cause' and **deformation response** is the
' effect'. Yet another parallel is the relationship between the electron distribution within the atoms of elements in the Periodic Table and such physical properties as the electrical and thermal conductivities, magnetic properties, etc.

It is now evident that central to the success of commercial units marketing materials for components is the need to appreciate the importance of producing an appropriate microstructure within the material. Two essential factors contribute to this. The first is the role of the material composition that has to be controlled to within close limits. The second is the processing of the material to the finished product.

Mild steels, for example, typically contain about
0.03-0.06 wt percent C
0.002-0.005 wt percent N_2
0.15-0.30 wt percent Mn
< 0.01 wt percent S & P
upto ~ 0.1 wt percent Si
A 300 tonne cast is produced within about 30 minutes of processing in a Basic Oxygen converter (BOS steel making). Within this period, the correct teeming composition has to be reached so that the ladle with the molten steel can travel to the continuous caster in readiness for casting . Often, alloying additions are also made to the melt in the converter. If extra strength is required in the steel, precisely calculated and controlled additions of P, Si, Mn, Nb, Ti are made to the melt. If, for example, resistance to atmospheric corrosion is required, controlled additions of Cu or Cr are made to the melt. If high temperature oxidation resistance is needed, precise additions of Ni are made to the melt. It is also important that these additions are thoroughly mixed in the melt. This is where an appreciation of physical chemistry , thermodynamics and

kinetics is required. An additional tool employed here is statistical process control. Given an awareness of these tools and the required experience, the melt has the correct composition and is now ready to be cast. Time after time, cast after cast, shift after shift , this procedure has to be followed in all the steel plants around the world.

Using mild steel as an example, the melt is now cast in the continuous caster. On solidification, as the strand emerges from the caster, it is cut into standard lengths. Typically, the slabs are about 10 meteres long, about 1000- 1400mm wide and about 250mm thick. The slabs are inspected for defects. They are then reheated to about
1200 ^{0} C in readiness for hot rolling. Hot rolling can be carried out to a final thickness of about 1.4mm at which stage the steel is at ~ 900^{0} C. It must be appreciated that the entire hot deformation ie from ~250mm down to ~1.4mm is carried out over the temperature range, 1200 to ~900 ^{0} C, ie when the steel is in the austenite phase ie. face centered cubic phase. The strip now runs over a cooling section ~100 m long where it is water cooled down to room temperature. This is where austenite transforms to ferrite, the body centered cubic phase. The strip is then coiled and cooled down to room temperature. Hot rolled strip , typically ~1.4 -10mm thick is sold to the market at various specifications.

When thinner gauges of sheet steel are required, for example, by the automotive sector, hot rolled coils are cleaned free of the oxide/ scale that forms on the surface of the sheet during hot rolling by a process called pickling. The strip , typically ~2.0mm thick, is then cold rolled to thinner gauges; to ~0.9-1.4mm for autobodies and ~0.15-0.3mm for the food packaging and the beverage can industries. This cold deformation workhardens the steel; it has to be softened by an annealing treatment to restore the ductility. Essentially, the sheet steel is now ready to be used for a wide variety of applications in the industry.

The above account clearly shows that processing entails several operations- continuous casting, hot rolling, pickling, cold rolling, annealing, etc. The key parameters here are, for example, the rate of casting, temperature, time at temperature, cooling rate, heating rate, amount of plastic strain (thickness reduction, for example, from 250mm to 1.4mm), strain rate (a function of the hot mill or cold mill speed), etc. Every one of these parameters has to be controlled to within precise ranges. Just as with the composition, discussed above, these parameters have to be reproduced time after time, coil after coil and shift after shift.

Commercial products are produced by a variety of methods : casting, forging, rolling, wire drawing, extrusion, welding, etc. Examples of some commercial products are shown in the following illustrations. Included amongst them is gold jewellery and a distribution chart showing the usage of gold. The role of the microstructure is just as important here as with the production of sheet steels described above. The following pages deal with specific examples of microstructures and their relevance to properties in materials.

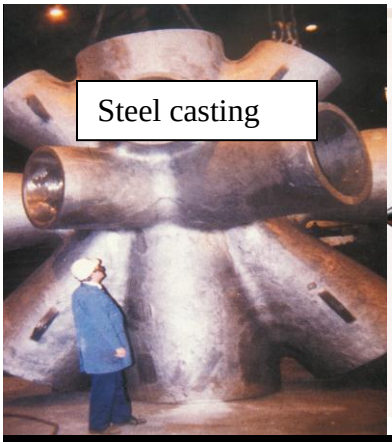

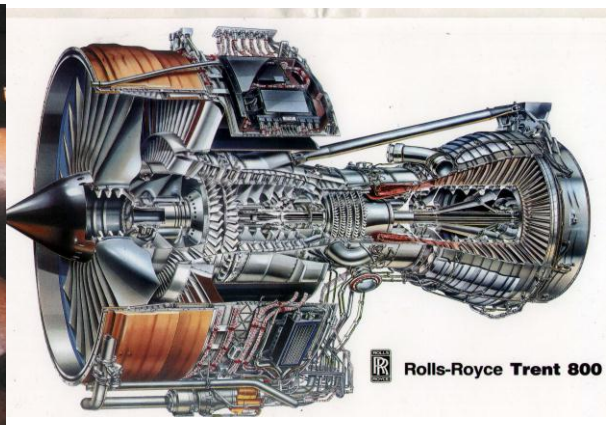

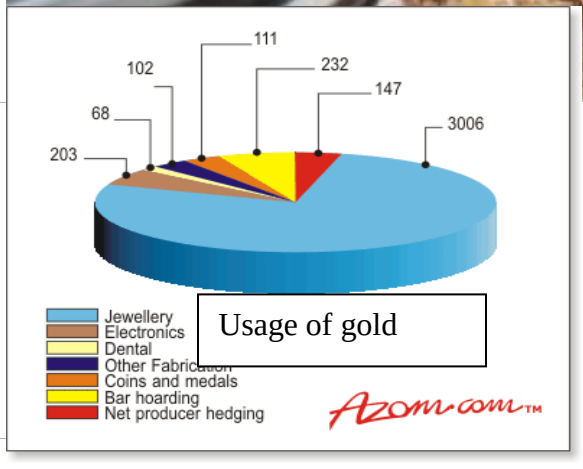

Fig 1.Examples of the applications of metallic materials

3. Microstructures in steels

3.1 Continuous casting

In sec 2, an example of a typical composition of mild steel and brief processing details are given in pages 5&6. The composition is reproduced here in relation to the Fe-C phase diagram. The inset shows the relevant part of the diagram relating to a mild steel.

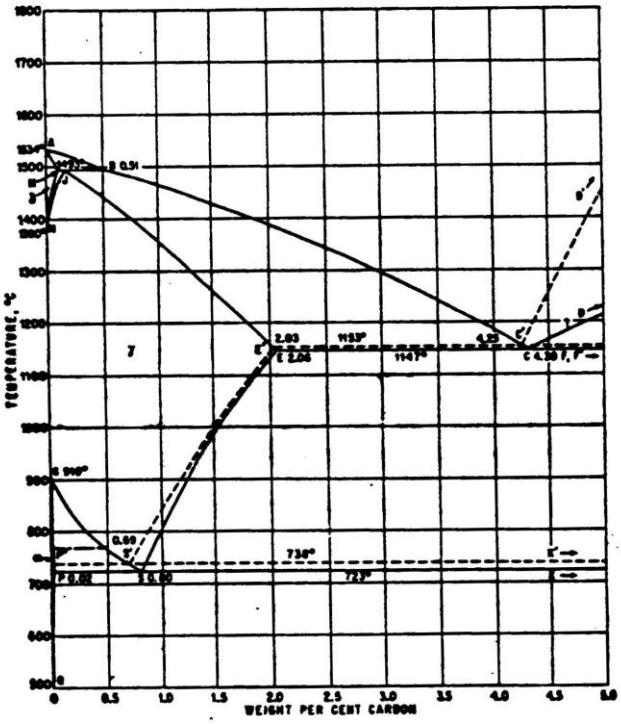

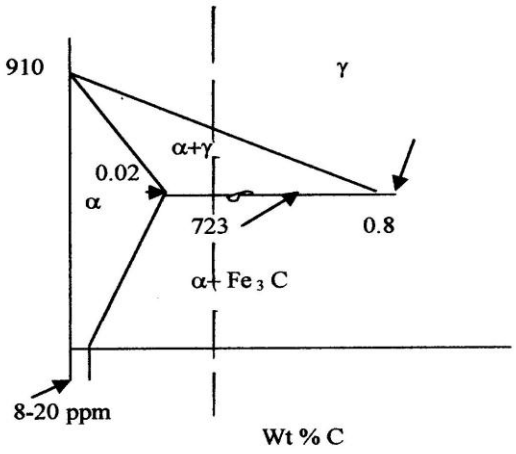

Figs 2&2a The Fe-C Phase diagram (from Hansen [2]) & inset of the α region

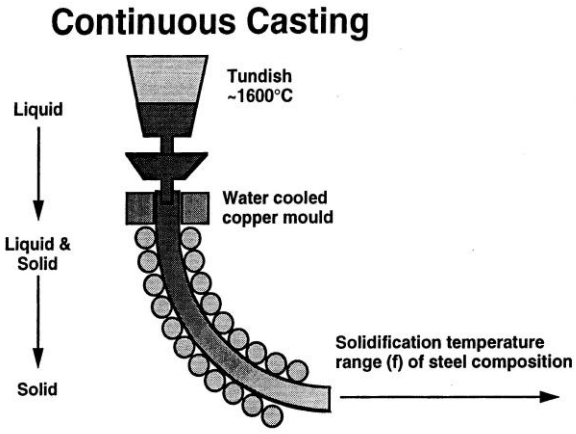

a. The copper mould (~900mm deep) facilitates the rapid solidification of the liquid steel.
b. Typical casting speed = ~0.9 - 1.0m/min.

Fig 3

Once the correct composition has been reached in the melt, the steel is emptied from the converter into a ladle. The ladle with about 300 tonnes of liquid steel at around 1400 ^{0} C is now transported to the continuous casting bay.

As the temperature drops, the steel goes through the liquid to liquid+solid to solid changes. Also, the steel goes through the various phase changes, culminating in the

γ to α phase change (Fig 2a). It is important to note that volume changes occur during cooling due to shrinkage as well as due to the phase change. Fig 4

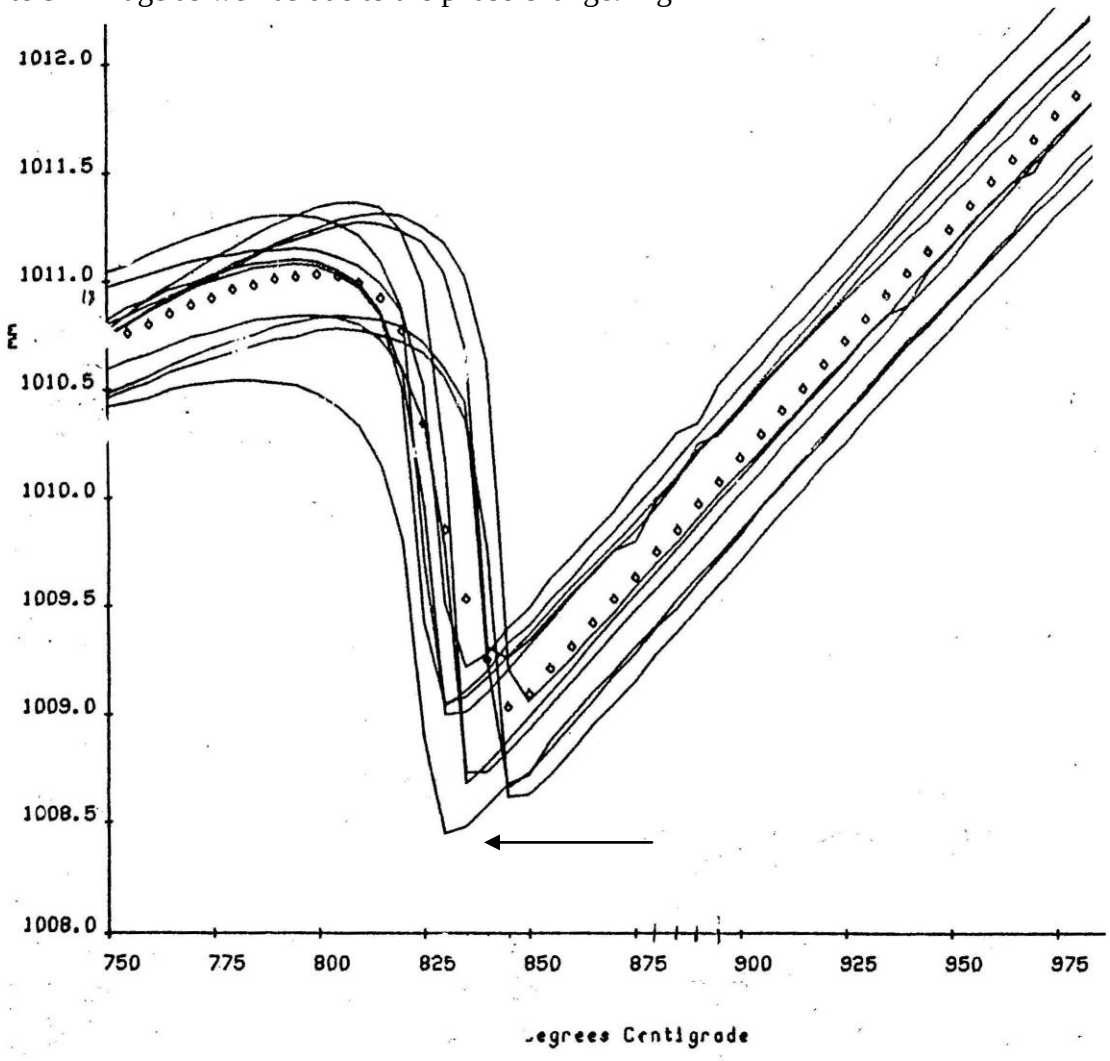

Fig 4. Dilatometer results ; dilation in mm (y-axis) vs temperature in degrees C (x-axis) (after P.Oldroyd/ Welsh Tech. Centre/Corus [3])

Fig 4 shows the cooling curves of a number of steels of different carbon levels, cooled over the range > 975 down to < 750 ^{0} C. It is seen that, over the temperature range of 850 to 825 ^{0} C, there is a significant expansion as γ transforms to α as the steel cools down . These volume changes can induce residual stresses on the slab as it emerges from the caster (Fig 3) and is cut into uniform lengths of ~10 metres by means of an oxy-acetylene torch. The residual stresses can induce defects and cracks on the slab; slabs are hence thoroughly inspected prior to being hot rolled.

Solidification of castings results in a microstructure similar to that seen in Figs. 5&6 a&b. The size of the dendrites depends on the cooling rates. Large sections such as continuously cast slabs (typically ~1400 to 1600 mm wide, ~250mm thick and ~10 metres long) cool slowly with the result that the as-cast structures show large dendritic areas. The initial chilling or rapid cooling of the molten steel on contact with the mould surface leads to fine equiaxed grains. This is

followed by the growth of the dendrites along the direction of the temperature gradient as solidification continues. Finally, the last pool of semi-solid metal solidifies into larger equiaxed grains. The three different families of dendritic crystals can be seen in Figs5 &6. Figs 6 & 6a show typical microstructures of continuously cast slabs.

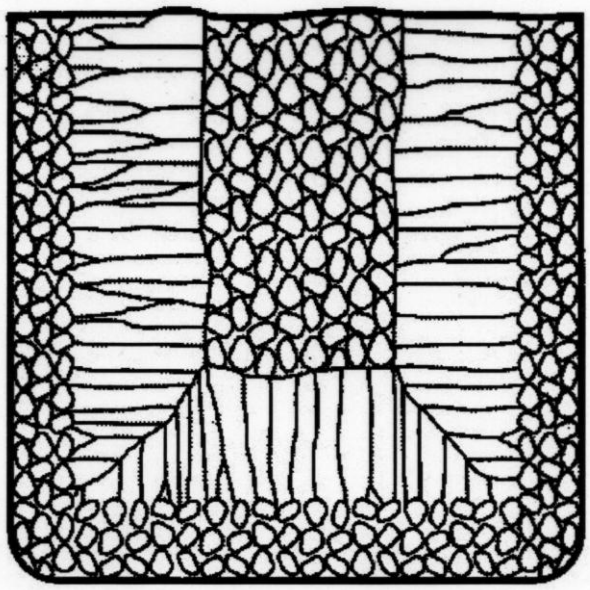

Fig 5. Schematic diagram of an as-cast structure (after R. Evans, Univ. Swansea [4])

Fig 6. Section of a con.cast slab

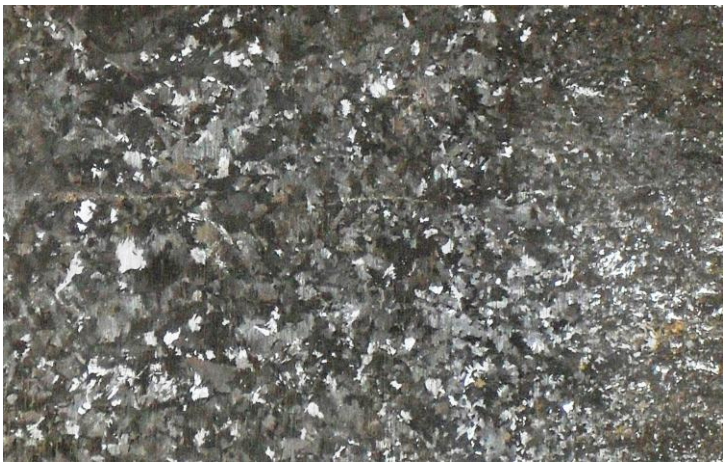

showing fine equi-axed ferrite grains

Following scarfing, cleaning and further inspection, the slabs are now transferred from the casting bay to the hot strip mill. They are now ready to be charged into the reheating furnace in preparation for hot rolling.

Fig 6a Section of a con cast steel slab

3.2 Hot rolling to sheet /strip.

The issues to be aware of are as follows.

1. the slab enters the first stage of rolling (known as 'roughing') at a thickness of ~ 250mm and at about 1200 ^{0} C.
2. it leaves this stage at t= ~90-100mm & ,after some delay (either on a 'delay table' or a 'coil box'), enters the 'finishing' mill at ~ 1000 ^{0} C (Fig 7)
3. it leaves the finishing mill at ~ 900 ^{0} C. At this stage, all the hot deformation has been completed and the strip thickness can vary, typically, from ~7 down to ~1.4 mm.

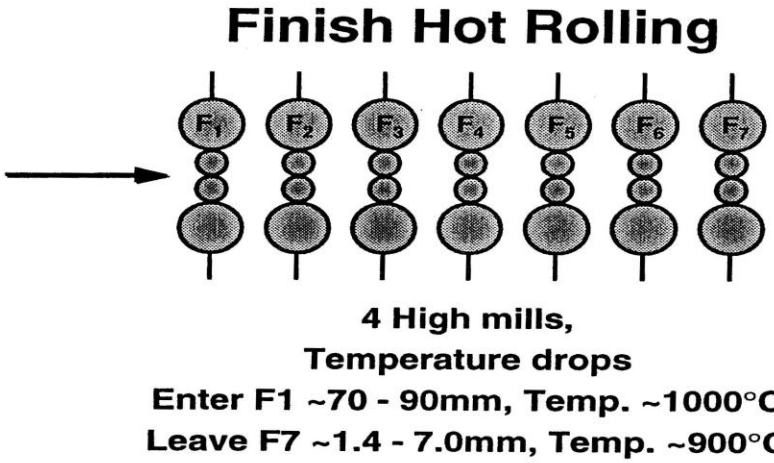

Dynamic recrystallisation prevents an increase in strength on rolling - Provided the temperature is greater than ~0.6Tm (where Tm is the melting point)

Fig 7. Schematic layout of the finishing section of a hot strip mill

4. all the hot deformation takes place whilst the steel is in the γ , austenite phase. (see Fig 2a). Austenite is face centered cubic (FCC) in crystal structure. FCC materials (Ag, Au, Al, Cu etc) have a multiplicity of slip systems and are easier to deform than body centered cubic materials (α iron, Cr, Mo, etc)
5. the hot deformation entails high levels of plastic strain (ε); the high mill speeds lead to hot deformation at high strain rates ($\dot{\varepsilon}$).
6. provided the temperature is high enough at a given stand (there are 7 seven stands shown in Fig 7), the steel will soften after accommodating a maximum amount of strain. This softening occurs by a process described as dynamic recovery or dynamic recrystallisation, depending on the stacking fault energy of the material. It is this process that occurs either instantaneously or between successive stands that renders the steel soft enough for further hot deformation in the following stand.

7. P.Richards [5] used an austenitic steel to study this feature. He chose this steel since
a. the steel was austenitic ie. it had a FCC crystal structure that was similar to the austenite phase (FCC) in a mild steel that is currently under study.
b. there was no γ to α phase transformation in this steel

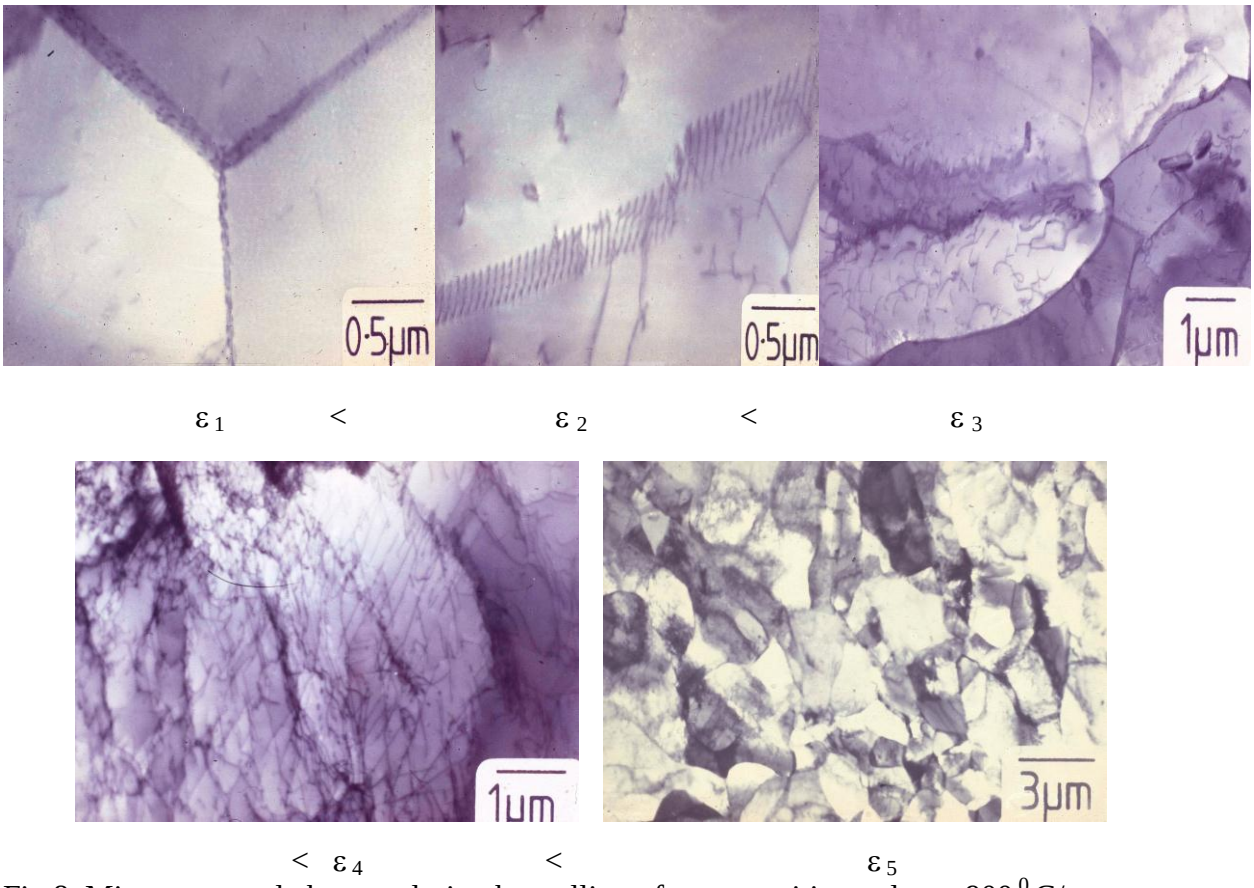

$\varepsilon_1 < \varepsilon_2 < \varepsilon_3 < \varepsilon_4 < \varepsilon_5$

Fig 8. Microstructural changes during hot rolling of an austenitic steel at > 900^0 C/ deformation temp.and the strain rate were constant in each test(after Paul Richards [5])

It is clear from the above sequence that as the rolling strain increases, the dislocation density increases until a point is reached where the strain exceeds a critical value and spontaneous recrystallisation is the outcome.

This implies that in commercial wide hot strip mills, softening can occur between stands provided the temperature and the level of plastic strain are high enough. However, as we move down towards the latter stands, the temperatures may not be high enough for recrystallisation to occur. It must also be noted that as the temperature drops on approaching the latter stands, precipitation can occur within the austenite, the effect of which would be to inhibit recrystallisation. The net outcome could be the onset of workhardening of the austenite phase.

3.3 Precipitation during hot rolling

The issues here are;

1. the phase in question is austenite, the γ , with the FCC crystal structure
2. FCC structures are more ‘’open’’ in the sense that they have a bigger solid solubility than ferrite, the α form, a BCC structure
3. the alloying additions made during steel making, eg, C,N, B reside in the interstitial sites and Al, Ti, Nb, etc reside in the substitutional sites within the FCC lattice
4. as we proceed from stand F1 to stand F7 (Fig 7), the temperature drops from about 1000 to ~900 ^{0} C.
5. the consequence of this drop in temperature is a fall in the solid solubility levels within austenite
6. the outcome is precipitation of such chemical combinations as Fe_3C, AlN, TiC, TiCN, NbC , NbCN etc.
7. this precipitation occurs concurrent with the hot deformation
8. such precipitation can lead to the steel becoming harder (thus requiring higher mill loads over those rolling stands where precipitation is expected)
9. such precipitation can also interfere with grainboundary migration, making recrystallisation more difficult
10. the combined effects of precipitation and the lack of recrystallisation towards the latter stands can lead to significant workhardening.

3.4 Cooling after the completion of hot rolling leads to phase transformation

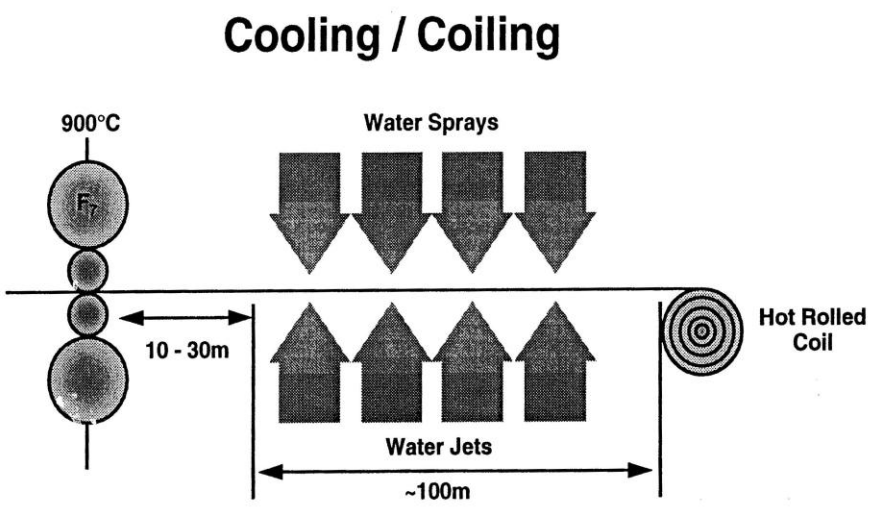

Fig 9. Cooling of the hot strip on the ‘run-out table ‘

Rate of cooling influences the grain structure and, hence, the properties. For example, very rapid cooling gives a fine structure and a strong product whilst slow cooling leads to a softer product i.e. lower yield/tensile strength

Fig 9 shows the cooling arrangement as the hot strip emerges from the last finishing stand at about 900^0 C. It is seen from Figs 2 &2a that austenite transforms to ferrite as the strip is cooled rapidly with the help of water sprays and jets over the run-out table which can be ~100 m long (Fig 7). It is clear from Fig 4 that this transformation occurs, in a number of steels with different carbon levels, over the temperature range of ~ $825\text{-}850^0$C.

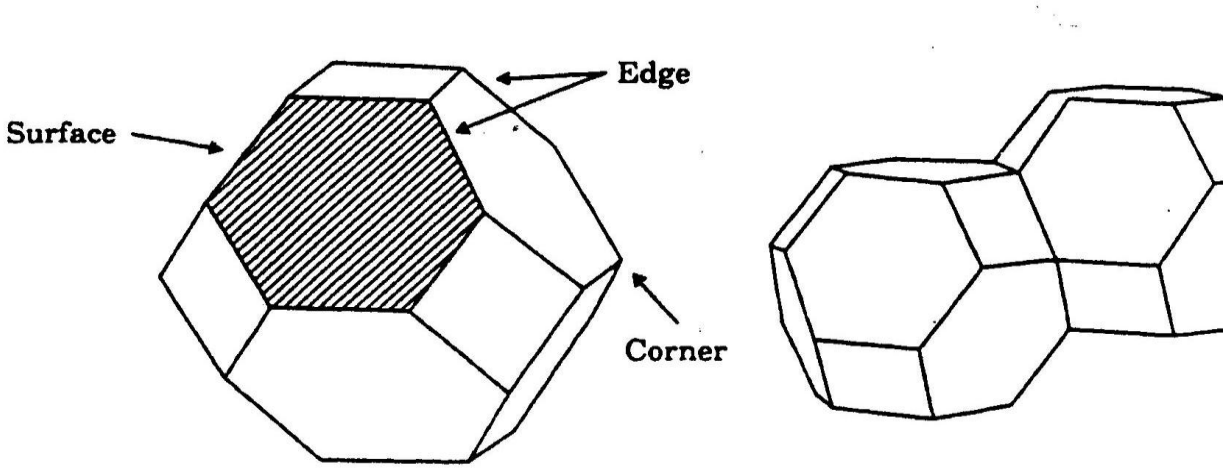

SCHEMATIC DIAGRAM OF A γ GRAIN AS A TETRAKAIDECAHEDRA AND SHOWING THREE TYPES OF NUCLEATION SITES OF α. ( )

Fig 10. Potential sites for the γ to α transformation

In theory, 27 potential ferrite grains can emerge from a single parent austenite grain (Fig 10) (see for ex. Ref 6). Transformation, hence, produces a significant refinement of grain size. With a high finishing temperature, the parent austenite grain size is large. Why ? Rates of self diffusion (diffusion of iron atoms) are temperature dependant and, hence, faster grain boundary migration leads to grain growth. Thus, despite the grain refinement, the ferrite grain size is large since the parent austenite grain size is large. The converse applies with a low finishing temperature. In extreme cases, as for example, at the tail end of a long coil, the temperature may be so low as to cross the phase boundary; the finishing temperature may lie in the two phase ($\alpha + \gamma$) region in Fig 2a. It is also possible that such low finishing temperatures may lead to incomplete recrystallisation of the austenite prior to transformation. The outcome of such differences in the finishing temperatures can lead to microstructural differences, examples of which are given in Fig 11. These mixed grain structures can, in turn, can lead to differences in mechanical properties. The outcome would be that parts of a coil may fall outside the specification.

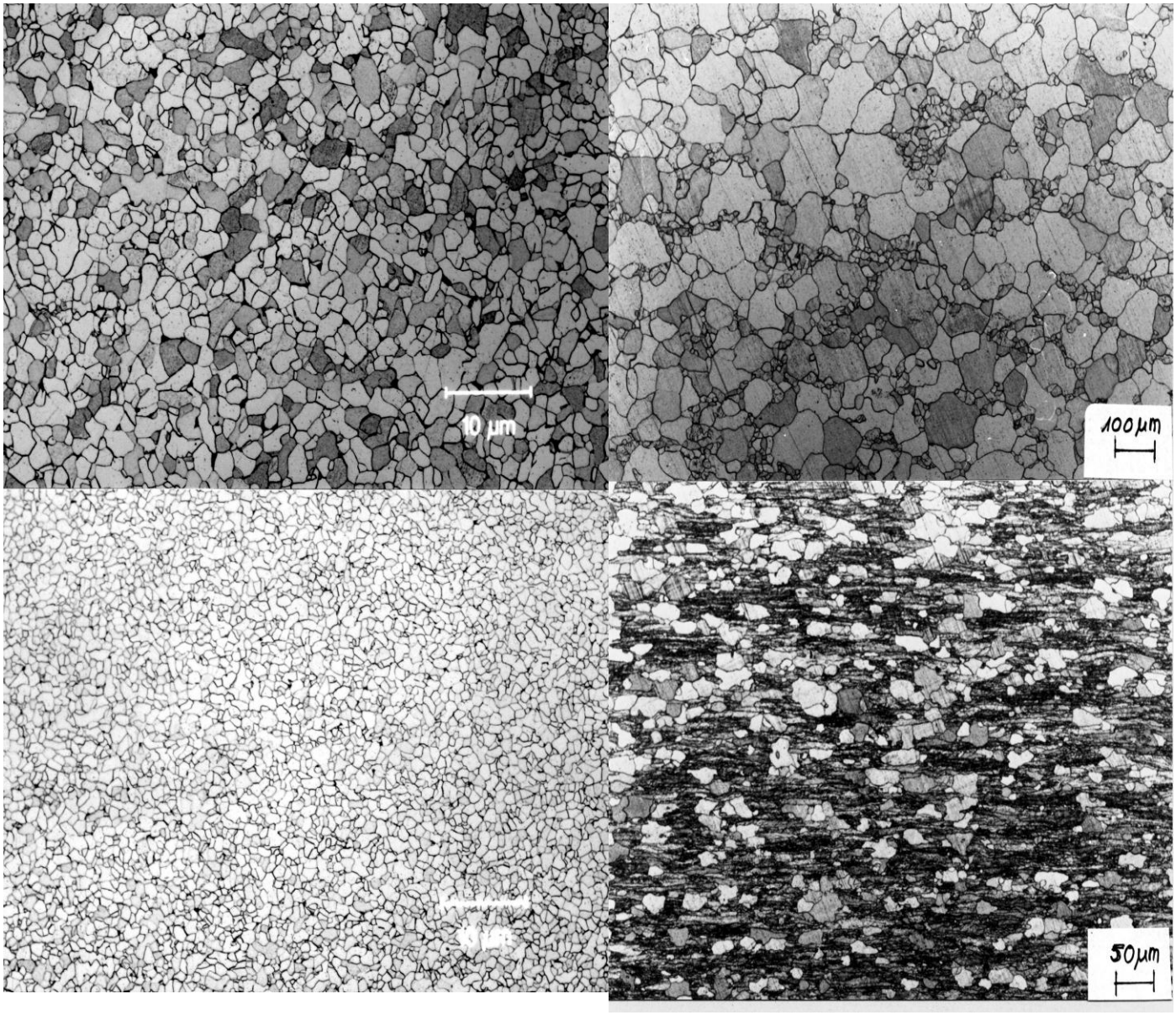

Fig 11. Effect of finishing temperature (FT) on the ferrite grain structure of hot rolled mild steel

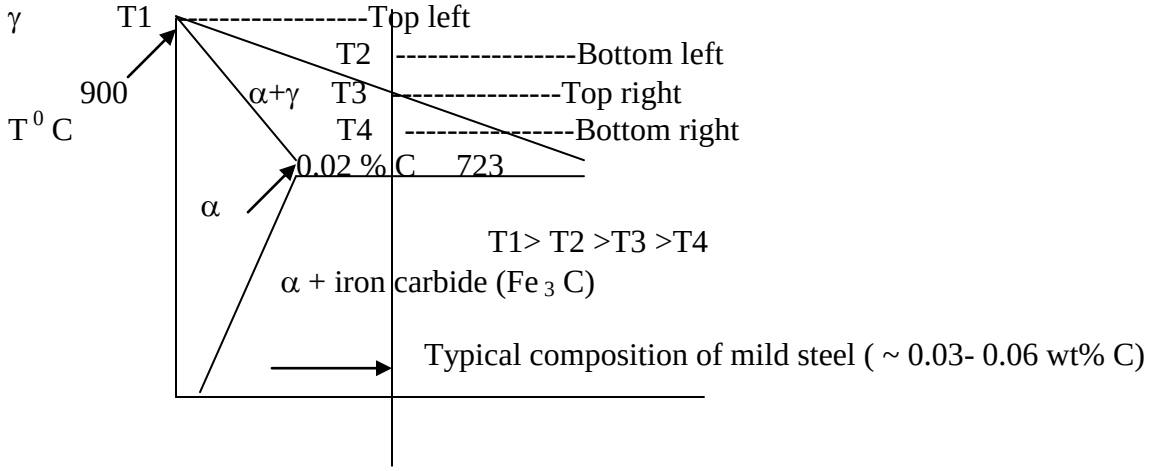

3.5 Precipitation observed in hot rolled steels

Depending on the grades, hot rolled coils are generally coiled over the temperature range 550 to over 700 ^{0} C. The γ (austenite) to α (ferrite) phase change causes a significant drop in the solid solubility levels. Further, the solubility levels in the ferrite decrease with temperature. Hence, those solutes that can not be retained in solution in the ferrite phase will precipitate out as chemical combinations of Fe and C as Fe_3C, Al and N as AlN, Ti and C plus N as TiCN, Nb and C plus N as NbCN, etc . The precipitates seen in the hot rolled state are hence a mixture of those that formed during the latter stages of hot rolling ie, in austenite as well those that formed in ferrite after the phase change. Figs 12 show examples of such precipitation.

Fig 12. Examples of precipitation and dislocation

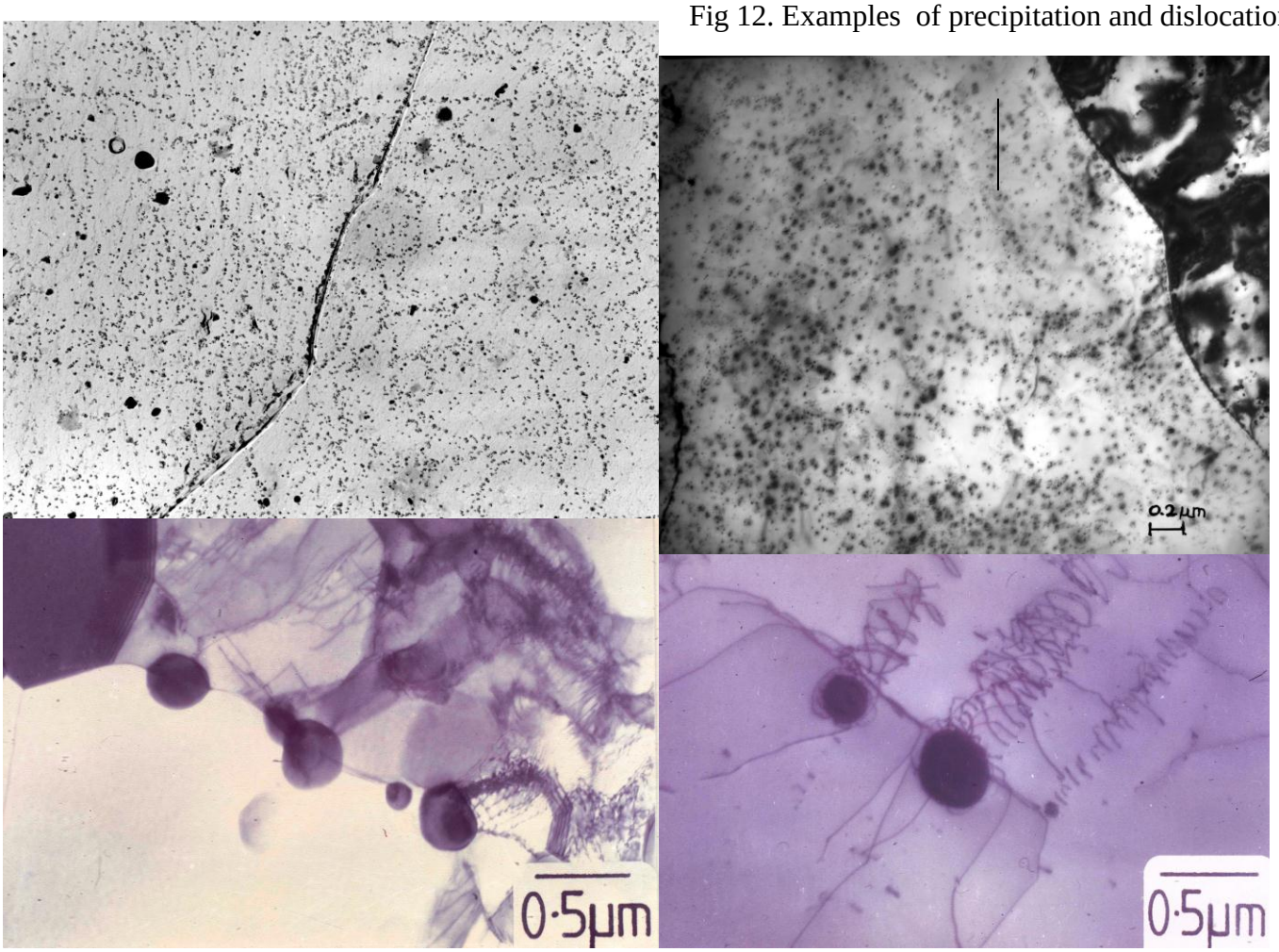

–precipitate interaction seen in hot rolled low carbon mild steels with small Ti and/ or Nb additions. (c& d [5])

a b

c d

a& b _____ 0.3µm

The precipitates seen in the figures are TiCN , NbCN and Fe_3C. Fig c shows the NbCN precipitates, < 0.5 μm in size, on the ferrite grain boundaries. They are very effective in restricting the growth of the ferrite grains by pinning the boundaries. Fig d shows the dislocation pile-up against NbCN precipitates. 'Grain refined high strength low alloy' steels (HSLA) employ this mechanism whereby the precipitates inhibit the grain growth in the ferrite as well as in the austenite prior to its transformation.

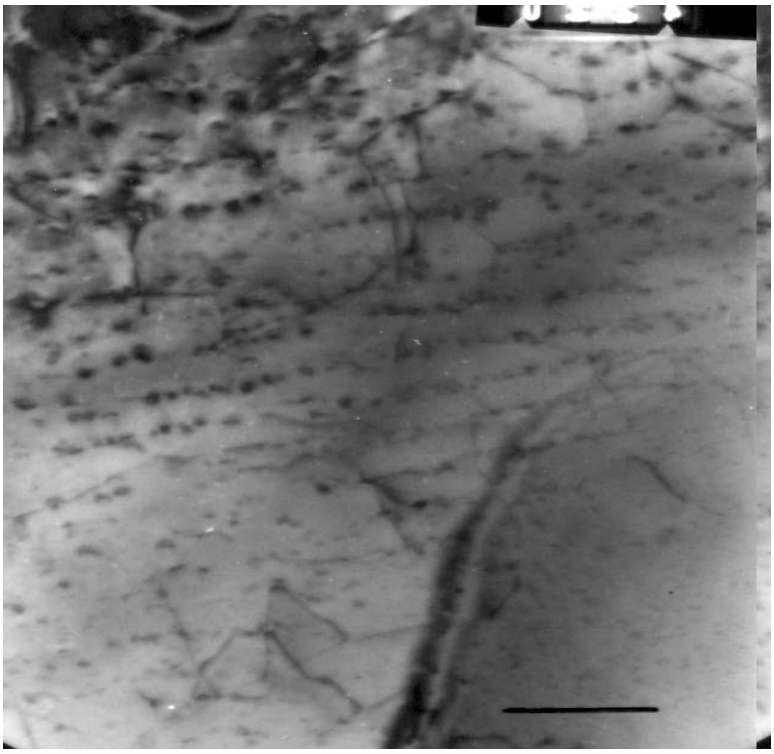

Fig 12e is an interesting example of the so called '' row type'' of precipitation of NbCN occurring at the austenite-ferrite interface as transformation progresses.
The fall in solubility levels as austenite transforms to ferrite leads to the rejection of solutes as precipitates in ferrite, this occurring at the interface.

(scale bar=0.2μm)

Fig 13

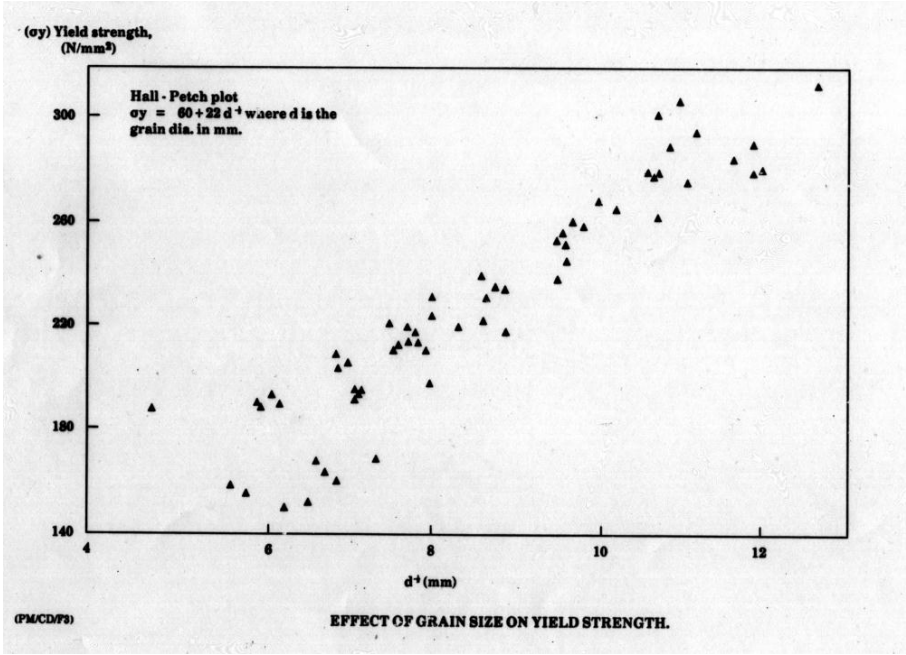

Fig 13 shows the effect of the ferrite grain size on the yield strength of steels. This is based on the work of Hall and Petch [7&8] and is reproduced by R.Evans. [9]

Hall and Petch found that the yield strength versus the grain size follows the relationship
$\sigma_y = 60 + 22\, d^{-½}$ (for low carbon mild steels)
where d is the ferrite grain diameter in mm.The grain size decreases as we move from left to right in the figure. It is evident that the yield strength increases as the grain size decreases.This is the basis of the 'grain refined high strength low alloy (HSLA) steels.

Less expensive versions are the C-Mn steels where higher C and Mn additions lead to enhanced strengths. (Fig 14) Somewhat more expensive is the dual phase steel where, by virtue of alloy additions such as Mo and/ or controlled hot rolling/ cooling after hot rolling, the microstructure is essentially ferrite with small amounts of bainite or martensite.(Fig 15). Significantly high strengths are a feature of this steel.

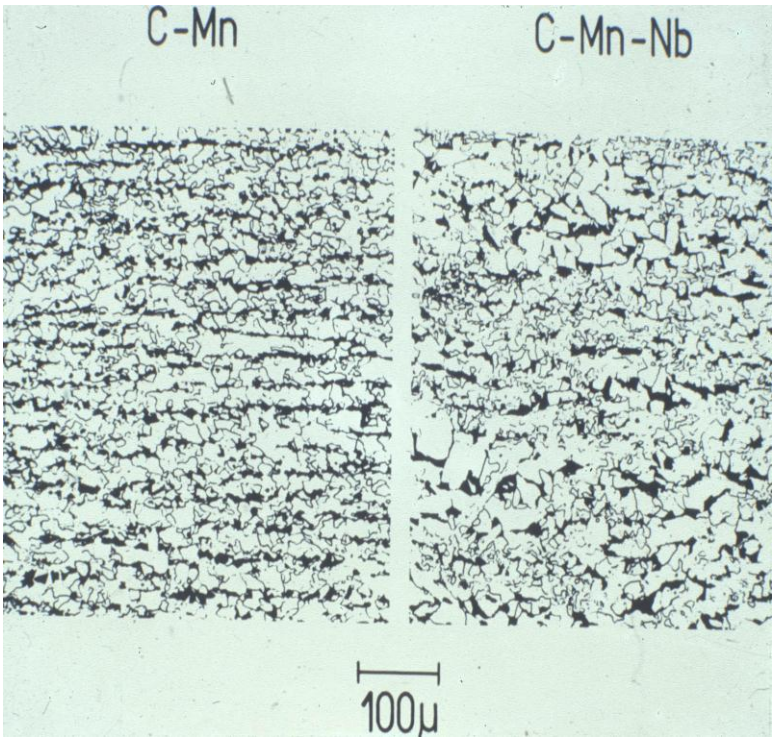

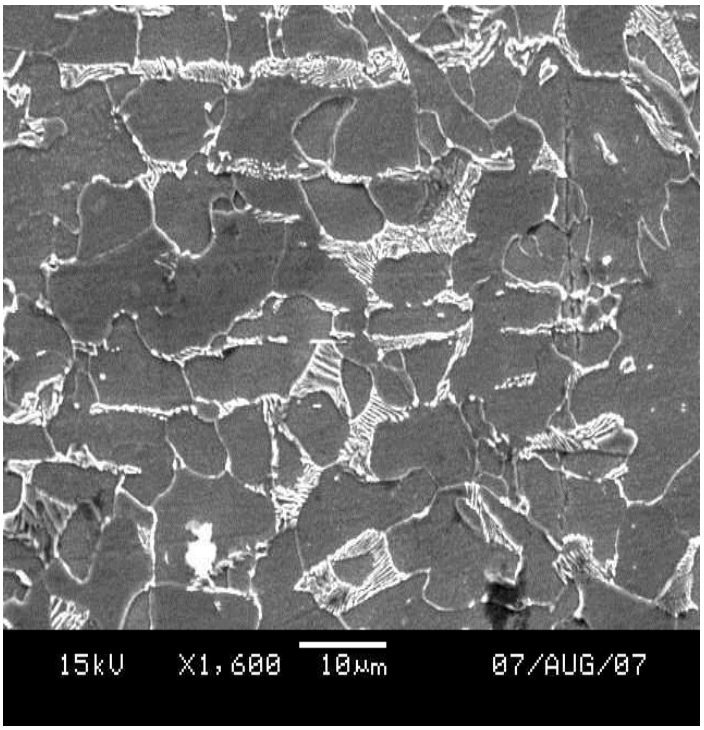

a b

Figs 14a C-Mn and C-Mn-Nb high strength steels showing ferrite and the dark regions of pearlite .

Fig14b/ 0.15% C & 0.8%Mn ferrite+pearlite/ after Phil Swanson, Coventry Univ)

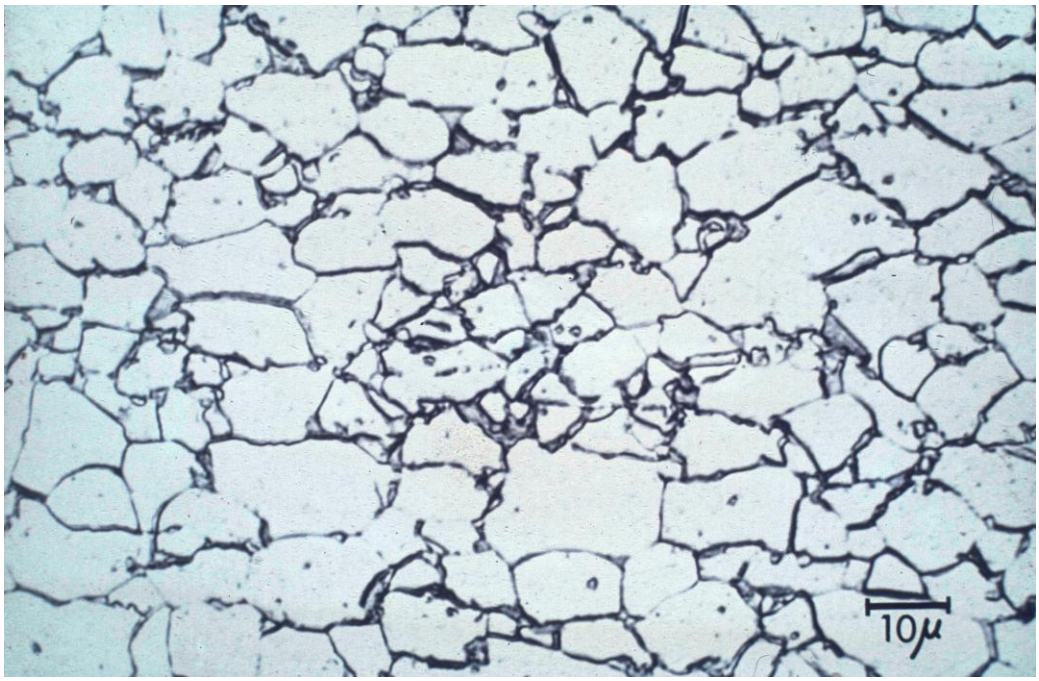

Fig 15. Dual phase steel. The light areas are ferrite and the dark areas are bainite or martensite.

The automotive industry, for example, is one of the key users of this grade. Indeed, it is probably fair to comment that it was at the behest of the automotive sector that this grade was developed. Dual phase steels are being widely used to replace the thicker sections based on mild steels with relatively thinner sections in order to reduce the weight of the components in the drive towards smaller engines and, hence, leaner emissions.

Fig 16 is a summary of all the essential issues involved in hot rolling of sheet steels.

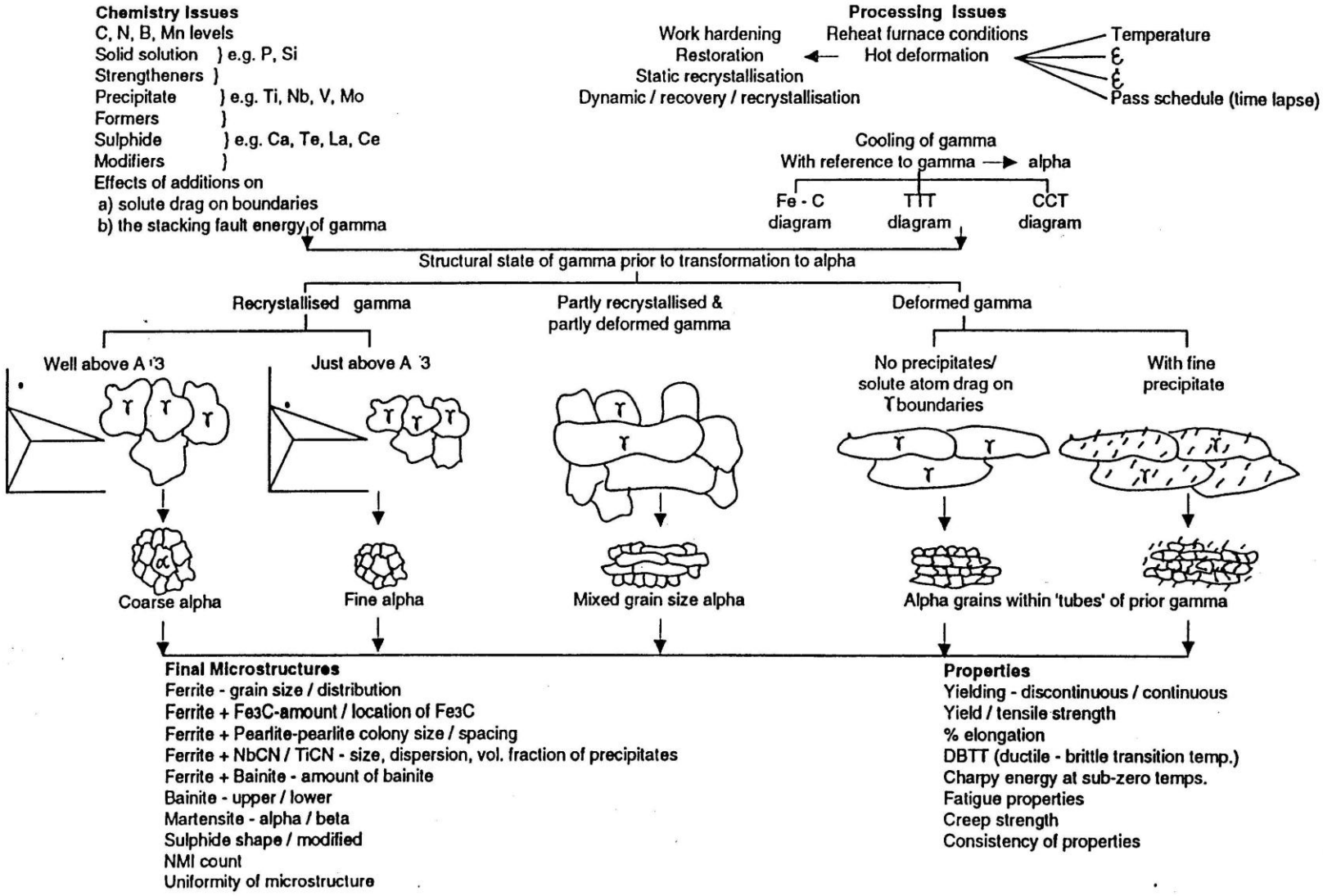

Fig 16. Schematic outline of the important aspects of hot rolling of sheet steels

3. 6. Microstructures of sheet steels after cold rolling and annealing

In normal practice, hot rolling of strip is limited to a final thickness of ~ 1.4 mm. If hot rolling were to be continued to a thickness < 1.4 mm, the strip temperatures will not be uniform across the width and along the length of a coil since the heat loss by radiation will be non -uniform and unpredictable. These temperature variations will produce gauge variations across the width and along the length of a coil as well as microstructural changes that lead to non-uniform properties. The steel will hence not meet the customer specification. Thinner gauge steels (< ~ 1.5mm) are hence produced by cold rolling the hot rolled strip, known as hotband, to the required gauges (Fig 17)

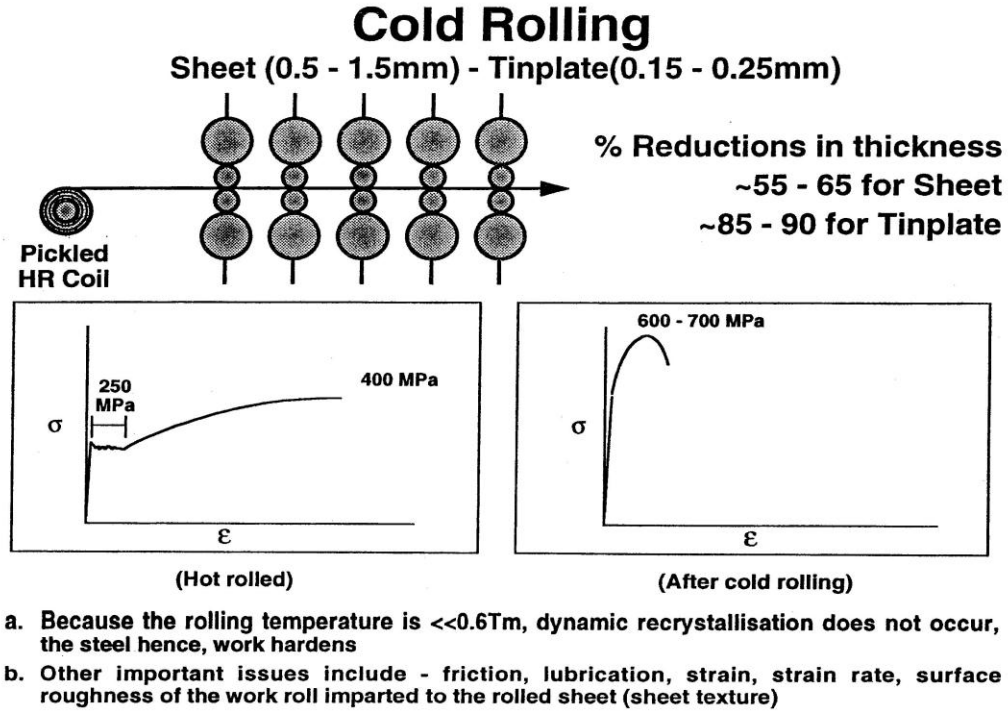

Fig 17. Schematic outline of the cold rolling of sheet steels

3.6.1 Microstructures and other features of the cold rolled steel

Fig 18 is an example of mild steel hotband microstructure. Its initial gauge, for example , is 2.00mm.On cold rolling to, for example, 0.65 mm, on the 5 stand/ 4 high cold mill (Fig 17), the changes are seen in Fig19. Ferrite grains in Fig19 are severely deformed and elongated along the rolling direction. The Fe_3C particles (dark areas) are broken into a dark debris on cold rolling.

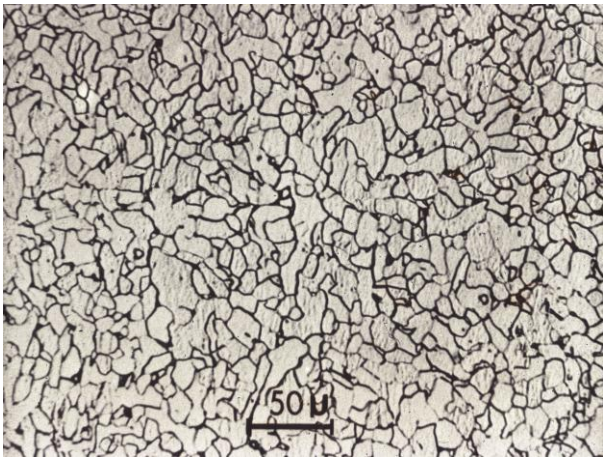

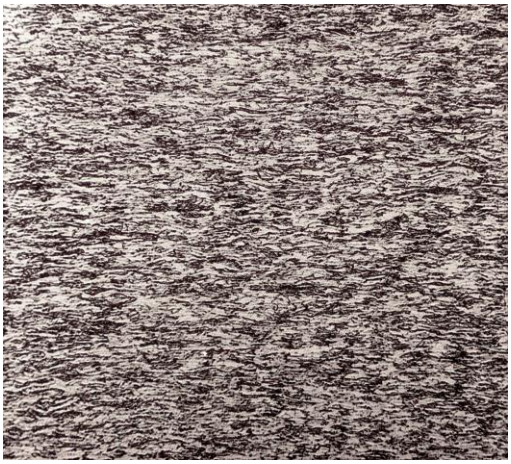

Fig 18. Mild steel hotband (t=2mm) Fig 19. After cold rolling (t=0.65mm) ------50µm

Cold rolling not only leads to a breakdown of the microstructure but also leads to 1. a high dislocation density 2.a significant amount of the stored energy of deformation 3. pronounced anisotropy. Deformation occurs via slip along the close-packed planes. In ferrite, a BCC structure, deformation occurs along preferred planes and crystallographic directions .The consequence is anisotropy ie. some regions are more heavily deformed and hence have higher levels of the stored energy of deformation than others. Thus, within the cold rolled strip, lie areas which are high energy orientations and those that are low energy orientations. It is also to be noted that anisotropy results in the bulk mechanical properties being different when measured along, across and at right angles to the rolling direction.

3.6.2 Annealing heat treatments of cold rolled strip

Essentially, this is a softening treatment (Fig 20),done on a batch basis or as a continuous

Fig 20

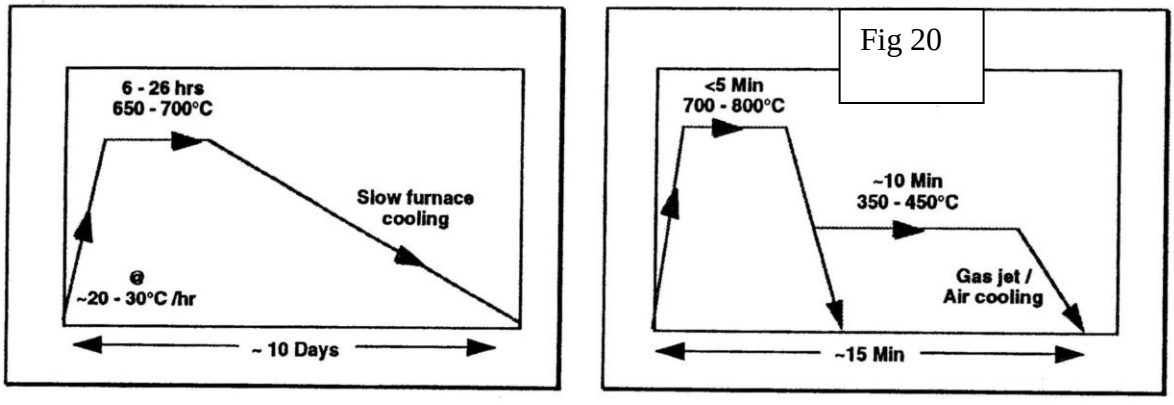

Annealing removes the effects of workhardening via recrystallisation, lowers the strength and restores ductility

treatment .The aims are to reduce the high dislocation density , to remove the microstructure seen in Fig 19, to induce recovery and recrystallisation , to reduce the high flow stress typical of a cold rolled material and to restore the ductility and other forming properties. The driving force for the microstructural changes comes from the stored energy of deformation, which, as we have seen already, is strongly orientation dependant. The high energy orientations such as { 110 } < uvw >, { 111} <uvw> are the first to recover and recrystallise, well ahead of such low energy orientations as { 100 } <uvw>,etc. Fig 21 shows the line broadening/sharpening data based on a low carbon steel. Line sharpening sets in at as early as from 300 ^{0} C in the high energy orientations such as { 110} and{222} orientations relative to the low energy orientations in the figure. This implies that recovery and recrystallisation set in sooner in the high energy orientations. It is the high stored energy of cold rolling in these orientations that provides the driving force for these microstructural changes such as dislocation annihilation that lead to the formation of nuclei and their growth in to recrystallised grains. The activation energy for recovery compares well with the activation energy for self diffusion in α iron.

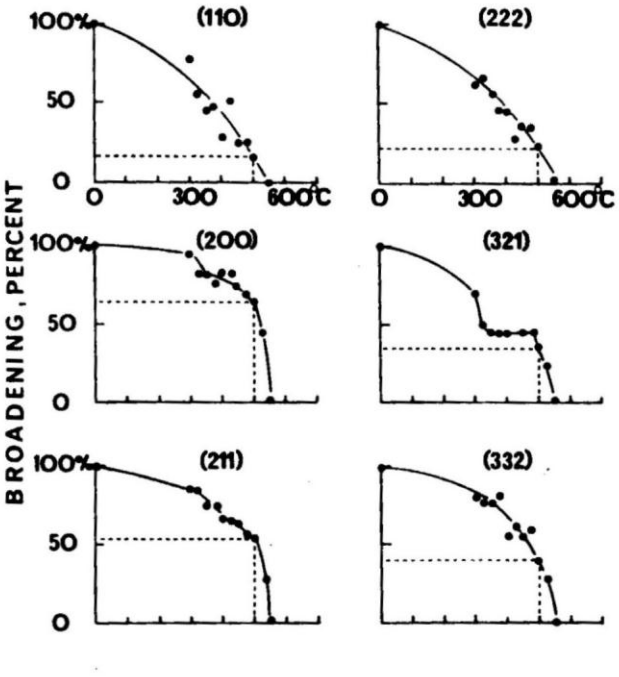

Fig 21 X-ray line broadening data (Dasarathy& Hudd [10])

Fig 22 relates to a specimen heated to ~500 ^{0} C and shows a recrystallised grain within an area that is not yet recrystallised. Diffraction evidence found this grain to be of the {111} < uvw> type of orientation ie. a high energy orientation. It is seen that the recrystallised grain is surrounded by an area with a high dislocation density. It is evident that the stored energy of this orientation was responsible for such early recrystallisation at a temperature as low as 500 ^{0}C.

-------- 0. 3μm

Fig 22. Microstructure of a low carbon steel slowly heated to 500 ^{0} C (after Adrian Dunn/ Univ.Liverpool [11])

Apart from the 'matrix' nucleation that is driven by the high stored energy, seen above, nucleation can also take place on the cold rolled grain boundaries (Fig 23) as well as in the proximity of large second phase particles such as iron carbides (Fig 24).

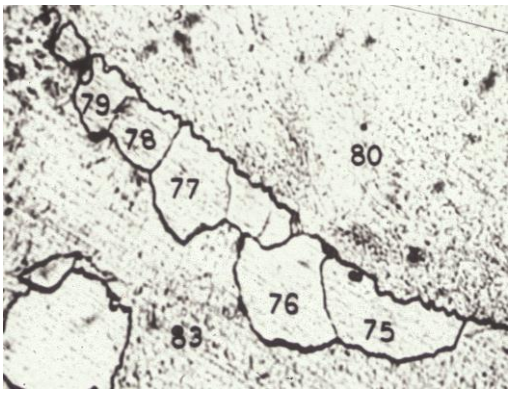

Fig 23, Nucleation at grainboundary (after Adrian Dunn/ Univ. Liverpool [11])

Fig 24,Nucleation aided by a Fe_3C particle (after D. T. Gawne [12])

In summary, nucleation of recrystallisation can occur in the matrix of a heavily deformed area; this is driven by the high stored energy and the orientations are usually of the {111}type. Nucleation of other orientations are aided by the presence of grain boundaries as well as second phase particles such as carbides; in these cases, stored energy levels are much less significant.

-------- 100μm

Fig 25. Onset of recrystallisation amidst a debris of elongated cold rolled grains

Fig 26. Sample in Fig 25 held for a longer time at a higher temperature to ensure complete recrystallisation

Annealing for a longer time or at a higher temperature leads to a significant growth in the ferrite grain size. Faster self- diffusion rates at higher temperatures lead to more vigorous grainboundary migration; the outcome is one of grain coarsening. (Fig 27). Of the two major variables that affect the speed of recrystallisation and grain growth, temperature is more effective than time.

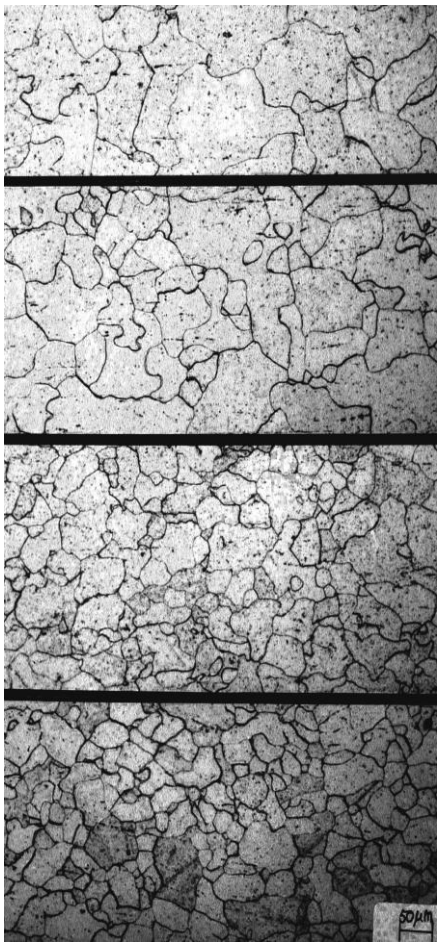

T4

-------- 100μm

T3

Fig 27 Examples of the effect of annealing temperatures on the grainsize. Samples were annealed for a constant time at the given temperatures

T4>T3>T2>T1

T2

According to Fig 13, the yield strength (YS) follows the order

$YS_1 > YS_2 > YS_3 > YS_4$

T1

It is important to note in Fig 20 that the annealing is carried out at sub-critical temperatures ie below ~723 ^{0} C; there is no phase transformation. It is the ferrite that changes from the deformed state to the recrystallised state. Batch annealing entails slow heating to temperatures < ~ 710 ^{0} C (from 600- ~700 ^{0} C) and holding for different times, depending upon the final grain size and hence, the strength levels required. Continuous annealing entails rapid heating, a short hold and , hence, a much shorter processing time. This requires higher annealing temperatures (~750 ^{0} C, for example) as well as for the carbon level to be < ~ 0.02 wt %, (see Figs 2a & 11). With carbon levels < 0.02 wt %, there is no danger of annealing in the two phase ($\alpha + \gamma$) region . Also, in order to provide a higher driving force/ stored energy so as to accelerate recrystallisation and grain growth, cold reduction levels are ~70-80% if the strip is to be continuously annealed; in contrast, the cold reduction levels are ~55 -65% if the strip is intended for the batch annealing route.

3. 6.3. Precipitation during batch annealing of aluminium stabilised steels

Examples of precipitation in hot rolled steels have already been seen in Fig 12. Precipitation can also occur concurrently with recrystallisation during batch annealing of cold rolled steels. Aluminium stabilised steels usually contain ~ 0.03-0.08 wt% Al. These steels also contain ~ 0.002-0.005wt % N. At the end of hot rolling, when the steel is cooled on the run-out table, the γ - α phase change occurs. In theory, precipitation of AlN can occur in the ferrite phase. In practice, however, the strip is cooled rapidly by using a coiling temperature of ~ 550-600 ^{0} C. This measure prevents AlN precipitation in the ferrite phase of the hot rolled steel. Instead, Al and N are held in ferrite in a state of pseudo-equilibrium. Given the slightest impulse, Al will combine with N to form AlN precipitates. Fig 28 (after W.Jolley [13]) Fig 28

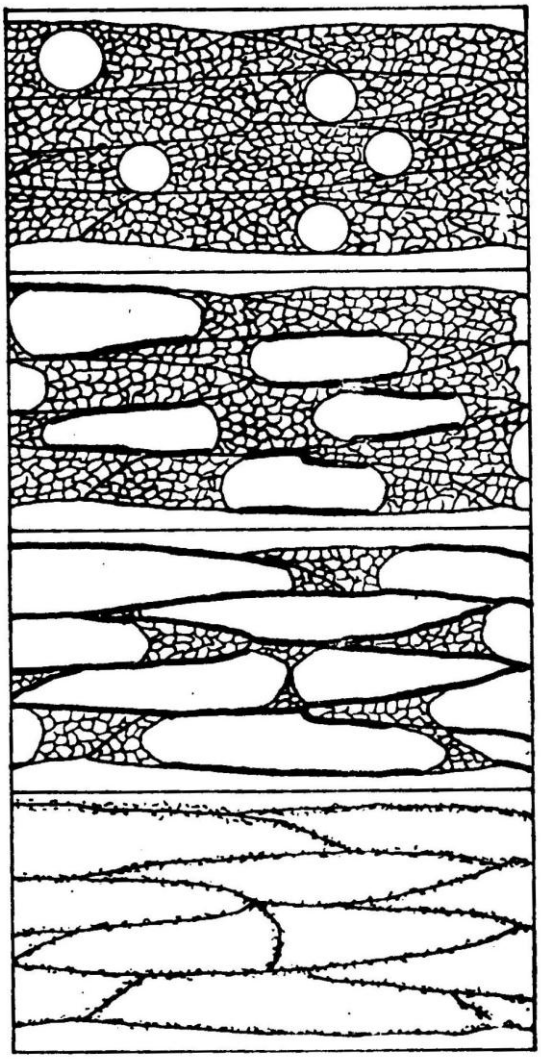

a. Recrystallised area first grows as equiaxed grain; aluminium and nitrogen at polygonized subgrain boundaries are 'swept up' as grain grows

b. Transverse growth is stopped because excessive aluminium and nitrogen concentration at as-rolled grain boundaries exerts too strong a drag on migrating boundaries

c. Longitudinal growth continues the recrystallisation process

d. Aluminium nitride precipitates at the former as-rolled (now recrystallised) grain boundaries

This impulse towards precipitation is given when the hot rolled steel is cold rolled and then batch annealed as in Fig 20. AlN precipitates concurrently with the progress of

recrystallisation. According to W. Jolley, pre- precipitation occurs on the grain boundaries of the cold worked grains .When recrystallisation begins, these clusters of Al and N atoms restrict grain growth along the thickness direction of the grains ; growth is hence, confined to the longitudinal direction of the grains. Microstructural evidence in support of this model is shown in Figs 29 , 30 &31. The onset and the completion of the development of this structure, known as 'pancake grains' is clearly evident in these figures.

Fig29

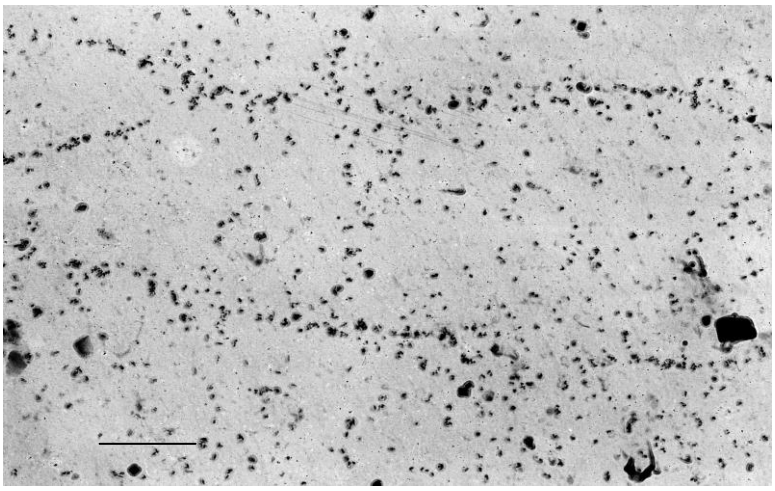

AlN precipitates along the recrystallising,elongated ferrite grain boundaries scale=0.3μm (similar to Jolley's model in Fig28 d)

Fig 30. Elongated recrystallised ferrite grains within the cold rolled structure

Fig 31. Fully recrystallised ferrite grains showing the 'pancake' structure

(scale=100μm)

3.6.4 The role of precipitates in secondary recrystallisation in steels

The grainsize distribution in the recrystallised structure shown in Fig 26 is such that very few grains have a distinct size advantage relative to their neighbours. Hence, when they grow during a longer anneal, they assume a distribution shown in Fig 27. However, when the primary recrystallised grain structure can be held stable with the help of precipitates such as AlN or MnS at their grainboundaries, growth as in Fig 27 is prevented on a further anneal. Instead, those few grains that are larger than their neighbours or those boundaries that are more favourably oriented , now begin to grow at the expense of their neighbours , provided the precipitates are of an appropriate size.

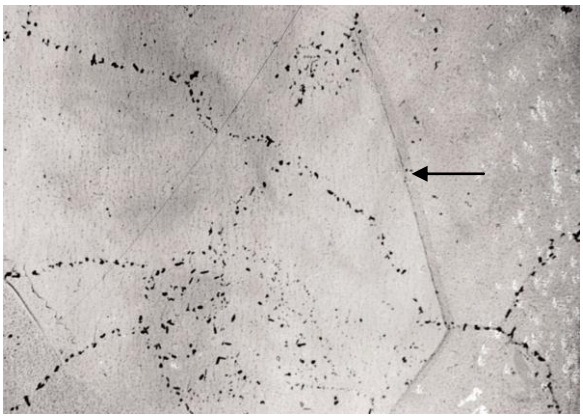

Fig 32. AlN precipitates outlining the recrystallised grains that existed prior to the onset of secondary recrystallisation. Arrow shows a part of the seccondary grainboundary (after Dasarathy& Hudd [14])

1μm

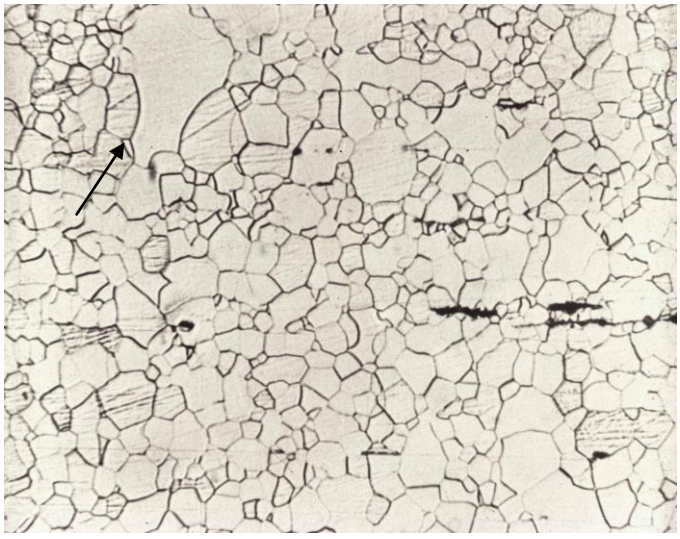

Fig 33. A large secondary grain is growing at the expense of its neighbours ,seen in an electrical steel with ~3% Si (see arrow)

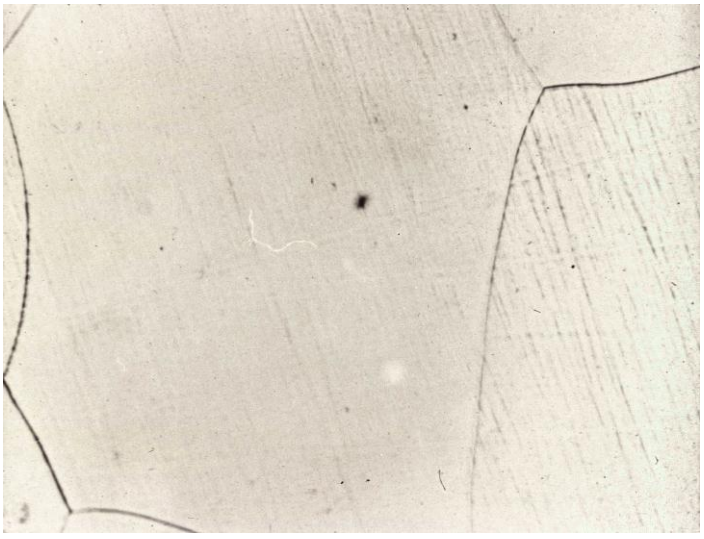

100μm

Fig 34. A large secondary grain seen in an electrical steel with ~3 % Si

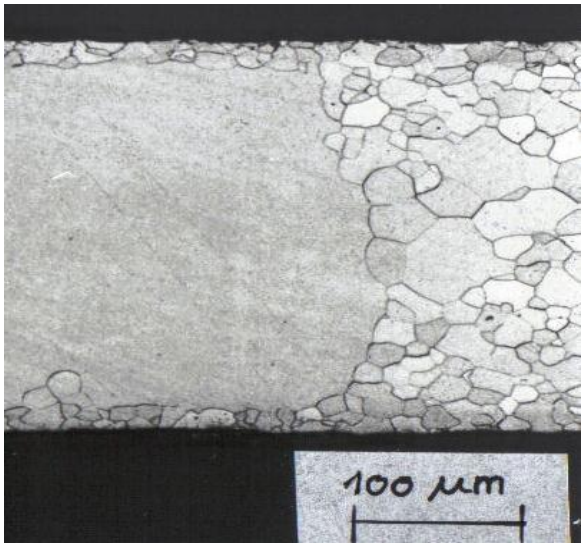

Fig 35 . A large secondary grain almost covering the sheet thickness

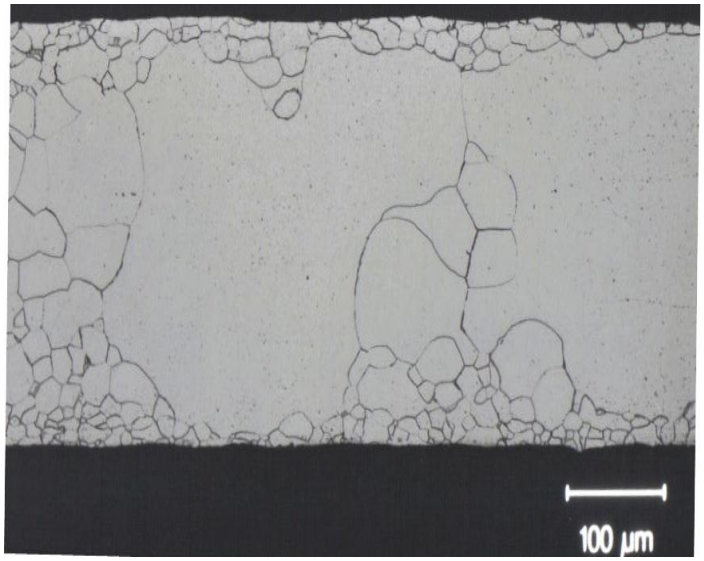

Fig 36 Large secondary grain consuming a few potential secondary grains (after Dasarathy & Hudd)

Initially, the dispersion of fine precipitates at the primary recrystallised grainboundaries is effective in pinning the boundaries and preventing grain growth. However, with a longer anneal or a second anneal, diffusion sets in, the precipitates coarsen, they grow in size, the inter-particle spacing increases, the restraint on grainboundary movement begins to ease; this is when and where the potential secondary grains break free of the constraint and grow at the expense of their neighbours as seen in the examples shown above.

Smallman [15] notes that during such abnormal growth, boundary movement will occur to achieve 120^0 at the boundaries ; the resulting movement of the triple point leads to the dihedral angles of $\sim 120^0$ at each junction. The outcome is a severe curvature in segments of the boundaries , see Fig 34-36. **Boundaries migrate towards their centres of curvature [15].** This , in turn, leads to further growth of the large secondary grain which, by now, is well established.

Fig 37 shows the x-ray inverse pole figure data measured on the samples at the surface as well as at mid-thickness levels. It is clear that secondary recrystallisation results in the preferential growth of the $\{111\} < uvw >$ type of grains. The large secondary grains seen in the above figures are of this type of orientation.

In the case of electrical steels that contain ~3% Si, we have already noted that MnS particles hold the primary recrystallised grain size essentially stable; this is similar to the role of the AlN precipitates seen above. Prior to the second stage high temperature anneal, the primary grains are of different orientations..

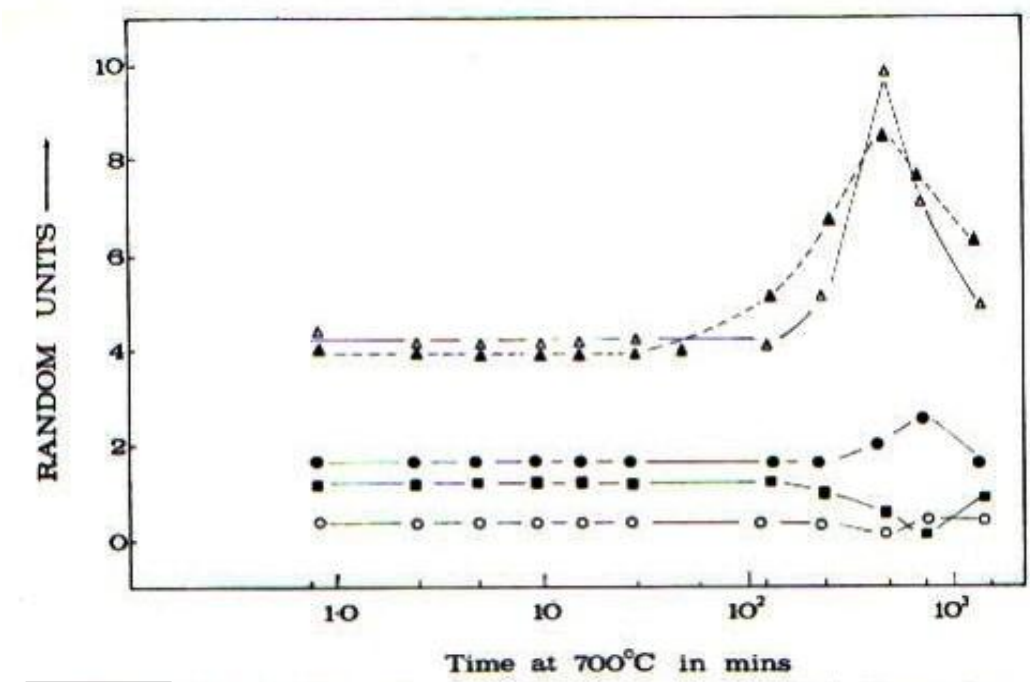

Fig 37 . Variation of texture components with time for samples annealed at 700°C.
Central section textures: △, (111); ●, (211); ■, (100); ○, (110). Surface texture: ▲, (111).

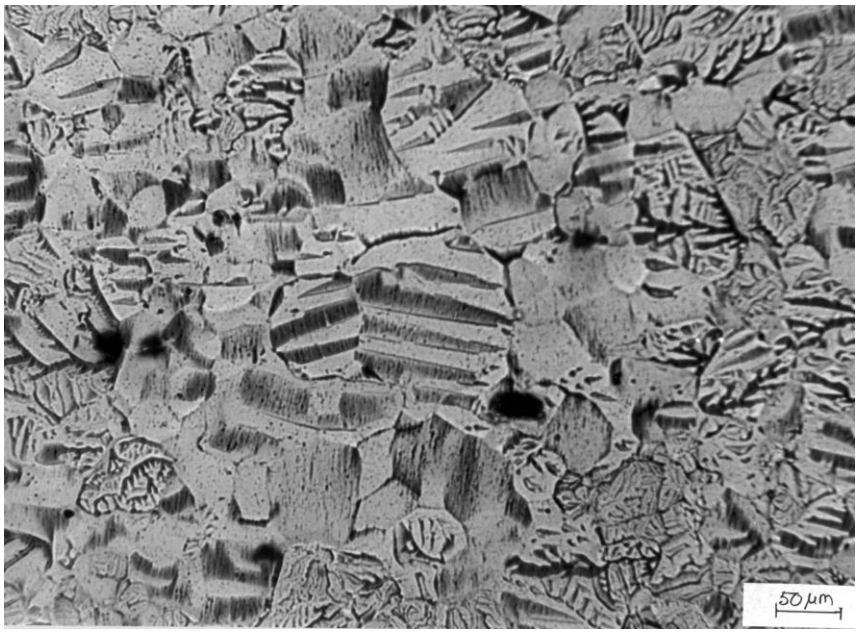

Fig 38 Magnetic domain boundaries in an electrical steel
(after P.Moore [16])

The primary grains are of different crytallographic orientations; the domain boundaries are aligned in different directions. A critical cold reduction folllowed by a decarburisation anneal and, finally, a high temperature anneal replace this structure with a few large secondary grains , often upto ~30mm in length: here the domain boundaries are aligned in essentially the same direction . This product is known as 'grain oriented Si steel' with a predominant {110} <uvw> type of texture , ideal for electrical applications.

3.6.5.Carbon precipitation on dislocations

Bake hardening steels are similar in compositon to an aluminium stabilised steel, except that the carbon is ~ 0.02 wt %. Fully processed steels , typically, have a 0.2% proof stress of ~ 170-180 N/mm^2. When automotive panels are formed out of these in the press shop, workhardening increases the flow stress by ~20-30 N/mm^2. The formed panels are then painted and baked, for example, at ~150-200 ^{0} C for ~15-25 minutes. During this paint baking treatment, carbon precipitation on dislocations (Fig 39) leads to a small increase in strength, typically, by ~20-30 N/mm^2. Thus, the overall strength (workhardening plus bake hardening) increase is about 40-60N/mm^2. This enhanced strength improves the dent resistance of the panels.

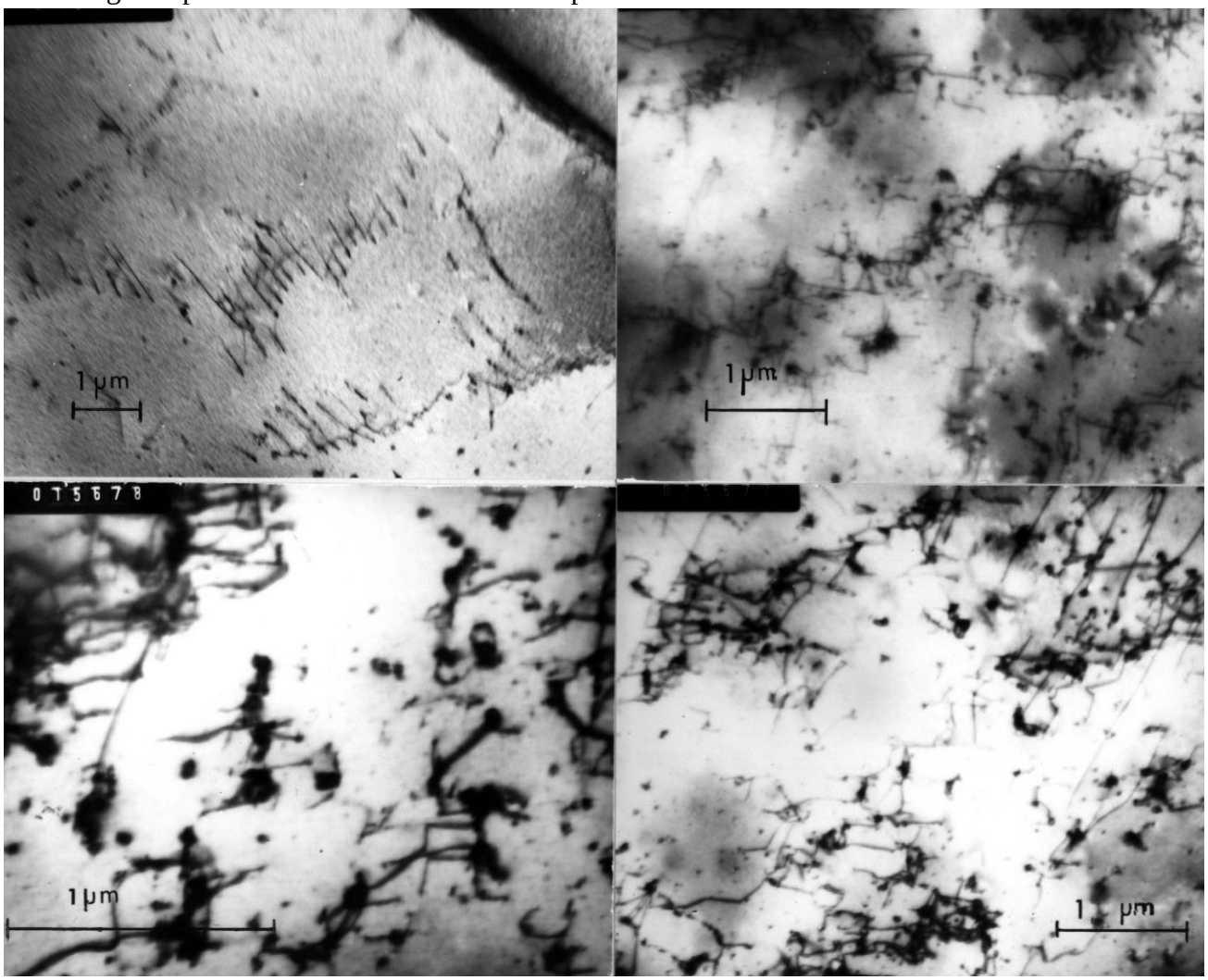

Fig 39. Microstructures after simulated bake hardening treatments
(after Lyons,Dasarathy & Hudd)

Bake hardening treatments are at low temperatures. Hence, the driving force for precipitation is low, thus ruling out the formation of Fe_3C. The best that can occur at these low temperatures and short times is for carbon to precipitate on the dislocations arising from the forming strains on the panels.In short,this is the basis of bake hardening.

3.7 Martensitic steels

Examples of means by which the strength of low carbon mild steels can be increased have been given in the previous sections. Briefly, the means availble have been

1. Interstitial solid solution strengthening with C, N,and B
2. Substitutional solid solution strengthening with P, Si,Mn
3. Grain refined High Strength Low Alloy (HSLA) steels with NbCN &/or TiCN precipitates which help to keep the austenite grainsize relatively small prior to transformation to ferrite on the run-out table
4. with the help of a finishing temperature that lies close to the γ - α transformation temperature; this results in a fine ferrite grain size
5. with the help of rapid cooling ie. using a low coiling temperature to produce a fine ferrite grain size
6. precipitation strengthening via NbCN or TiCN – dislocation interaction
7. By controlling the carbon level, bake hardening steels acquire an increase in strength whilst the formed automotive panels are given a paint baking heat treament at a low temperature, typically ~ 150-250 ^{0} C. This increase comes from carbon precipitation on the dislocations that arise from the forming strains in the material.
8. Controlling the cooling regime on the run-out table so that a large part of the austenite transforms to ferrite and the residual austenite transforms to bainite or martensite to produce the dual phase steels
9. TRIP (transformation reinforced plasticity) steels are a new addition where ,given suitable alloying and an appropriate cooling regime on the run-out table, the microstructure, essentially ferrite, also contains a small amount of residual austenite; this austenite transforms to martensite whilst undergoing plastic deformation during the forming of automotive components.

Having exhausted the above options , if higher strengths are still needed, rapid quenching of the austenite in water, brine or oil produces martensite. If , however, this practice is applied to sheet steels, the FCC to BCT(body centered tetragonal)transformation results in significant shape distortion. This is the reason why martensitic structures (Fig 41) are more often found , for example, in forged components than in sheet steel components. The fibrous apperance of the forged connecting rod can be seen in the macrostructure given in Fig 40/ from Internet.

Fig 40Fibrous grain flow

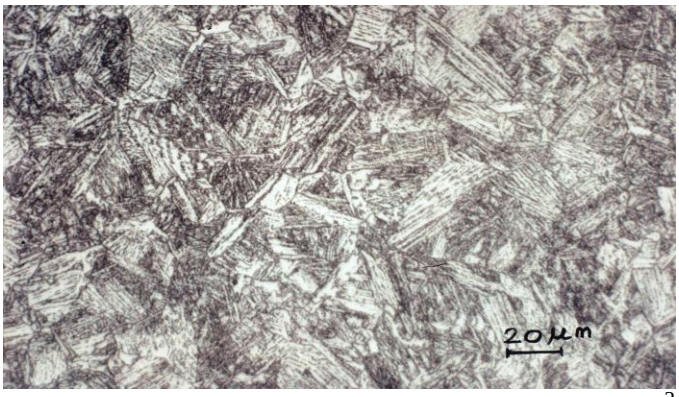

Fig 41. Martentisitic steel with a TS of ~700N/mm^2

3.8 Austenitic and Duplex stainless steels

Nickel and chromium, if added in sufficient amounts, can stabilise the austenite to such a degree that it remains stable right down to room temperature. Additions of up to ~ 18% Cr and about 8-10% Ni can result in austenitic stainless steels. The γ-α transformation is suppressed as a result; the steel is now non-ferromagnetic. Chromium additions provide enhanced corrosion resistance whilst nickel additions provide resistance to high temperature oxidation . Fig 42 shows an example of an austenitic stainles steel.

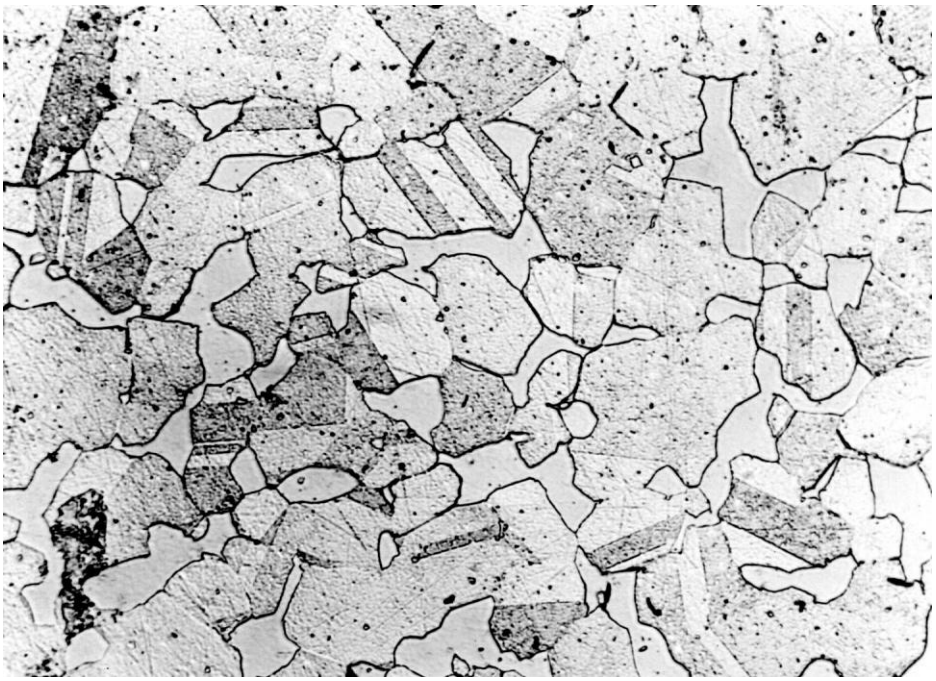

Fig 42. Annealed austentic stainless steel

Austenite is FCC in crystal structure. Annealing twins seen in Fig 42 are typical of those that occur in FCC based materials. Worked and annealed materials show extensive twinning [15] . Smallman notes that the best examples are seen where extensive grain growth has occurred. Twin bands grow in width during grain growth. With a low stacking fault energy metal such as copper, annealing twins are relatively common whilst they are rare in those with high stacking fault energy such as aluminium.

Typically, these steels contain ~0.08wt% C. They are relatively soft with superior formability, capable of being used for deep drawn components such as sinks, etc. Their principal limitation , however, is that they are particularly prone to stress corrosion cracking.

Duplex stainless steels show a mixture of ~50% austenite and ~50% ferrite in the microstructure. With leaner additions of Ni (~ 1-7%) , these steels are less expensive .

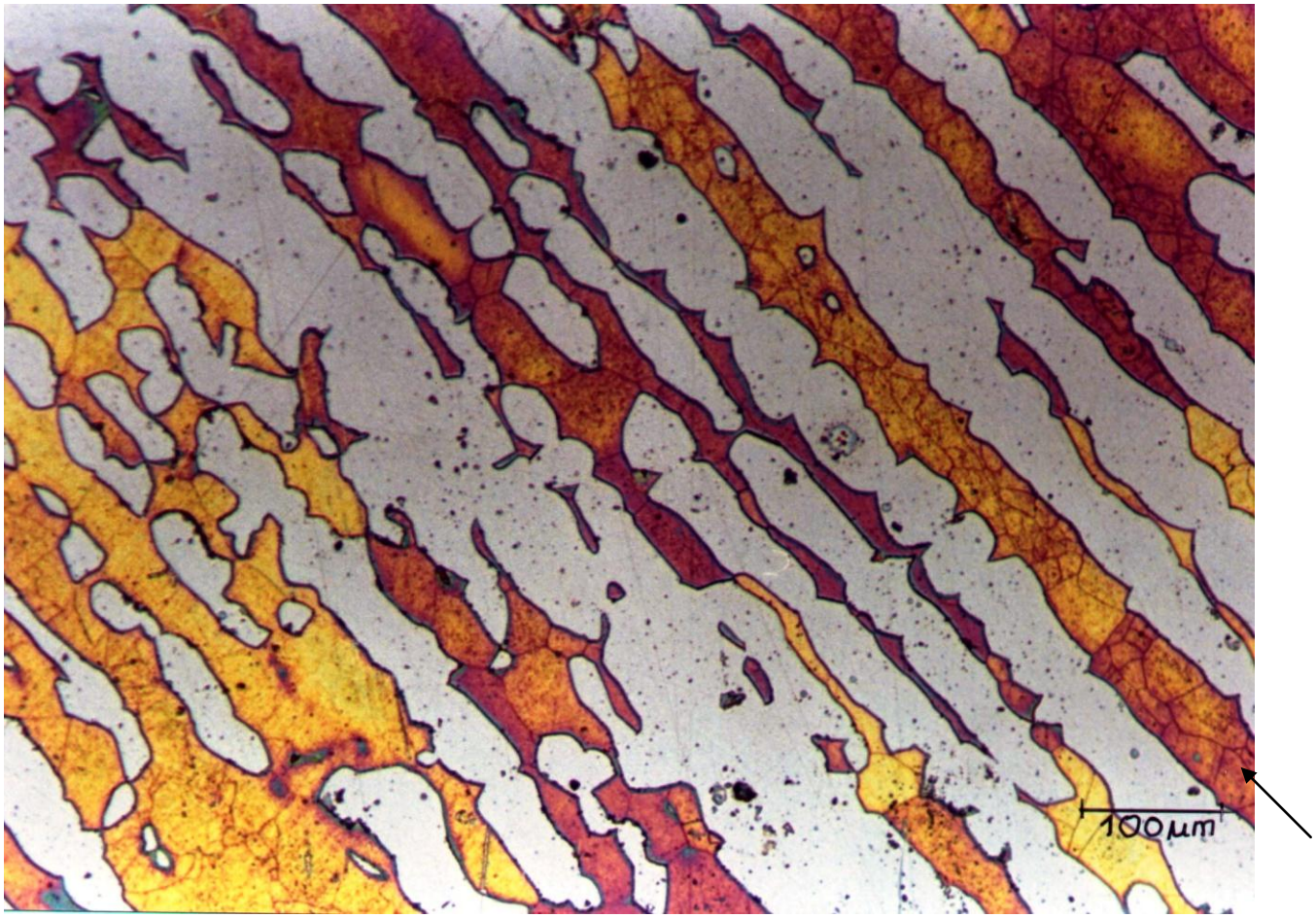

Fig 43.Microstructure of a duplex stainless steel. The coloured areas are ferrite and the matrix is austenite. Note the substructure within the ferrite regions shown by the arrow.

Typically, they contain ~20% Cr and small amounts of ferrite stabilisers such as Mo (~ 1-7%). Their yield strength (~400-500 N/mm^2) is roughly twice that of the austenitic version.As a result, their formability is poorer in comparison. Their higher strength enables the steel to be widely used in pressure vessels, etc in thinner sections in order to reduce the weight of the components.Another benefit is that the material is much less prone to stress corrsion cracking.

4. Deformation, recrystallisation and grainboundary migration in materials other than steels.

The sequence of examples given below follows the order of increasing deformation applied to materials prior to their recrystallisation.

4.1.**Very dilute alloys of indium with iron** were molten in recrystallised alumina crucibles under an argon atmosphere and slowly cooled from the liquid state down to room temperature. The Fe-In phase diagram shows a wide range of liquid immiscibilty, from ~3.4 to ~90 at % In. Fig 44. (Dasarathy [17,18])

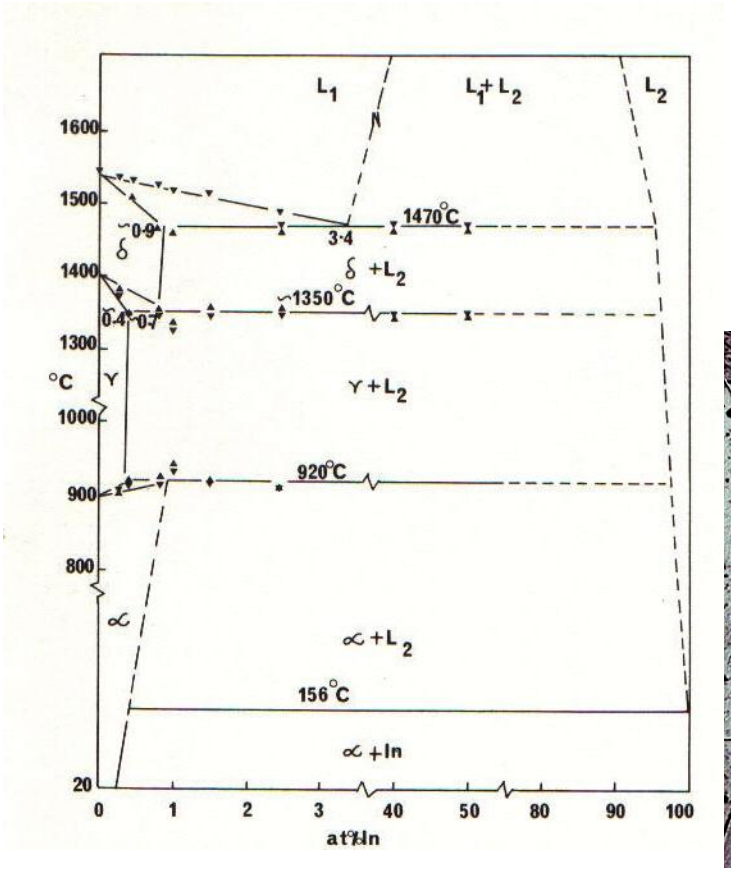

Fig 44 The Fe-In phase diagram.

The volume change (~1%) accompanying the γ to α phase change produced enough **transformation stresses** within the ferrite grains so as to develop a sub-grain structure, known as **alpha veining** . The transformation takes place in the presence of liquid L_2.Examples are given in Figs 45 &46.

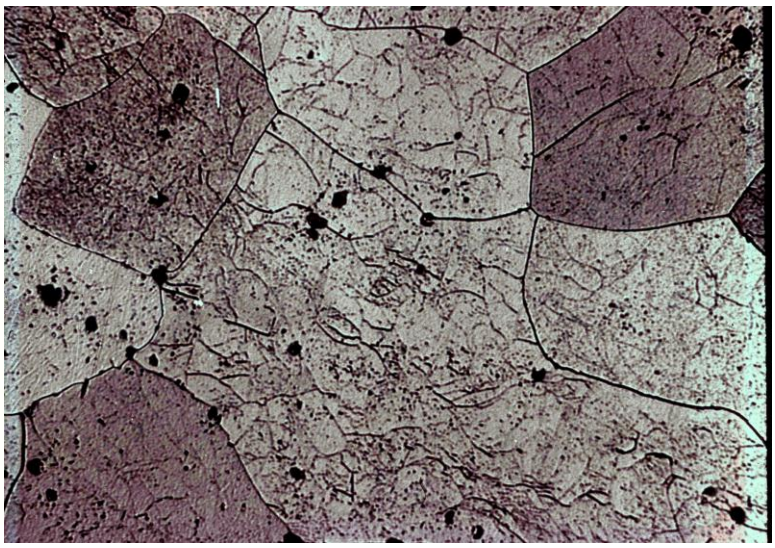

Figs 45 &46. Fe- ~2at % In alloys showing α veining(same mag)

Fig 45

Fig 47 . Annealing twins seen in the BCC ferrite grains in the Fe-In alloys

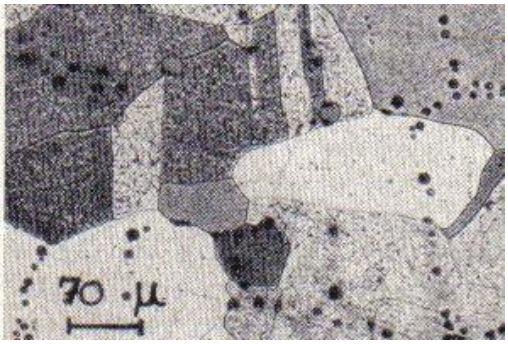

The examples given in Figs 45-47 show several interesting features;

i. in the high purity Fe-In alloys studied, the γ to α transformation occurs in the presence of liquid metal (L2)/Fig 44

ii. the volume change resulting from this transformation induces **plastic deformation** in the BCC ferrite phase; see also Fig 4 to appreciate the volume change involved in the γ to α phase change in steels

iii. The outcome of the deformation stresses is the appearance of sub-structures, known as alpha veining, within ferrite ; similar alpha veining has also been seen in high purity iron

iv. Whilst annealing twins are more often seen in FCC materials (see example in Fig 42), they are less frequent in BCC materials. Yet, Fig 47 shows annealing twins within the BCC ferrite grains.

4.2. The point of interest here is that **electron beam irradiation** can produce effects similar to **small amounts of plastic deformation** so as to trigger a burst of deformation/ mechanical twins.

Thin foils of **indium** were examined by transmission electron microscopy at 20^{0} C. Although there was a certain amount of dislocation movement, the significant observation was that twins nucleated and propagated. Typically, one or two twins were nucleated at first. This was closely followed by the nucleation , in a burst, of several twins in the vicinity, Fig 48. Some of the earlier twins broadened with time. Twins nucleated in the proximity of grain boundaries as well as at pre-existing twin boundaries.

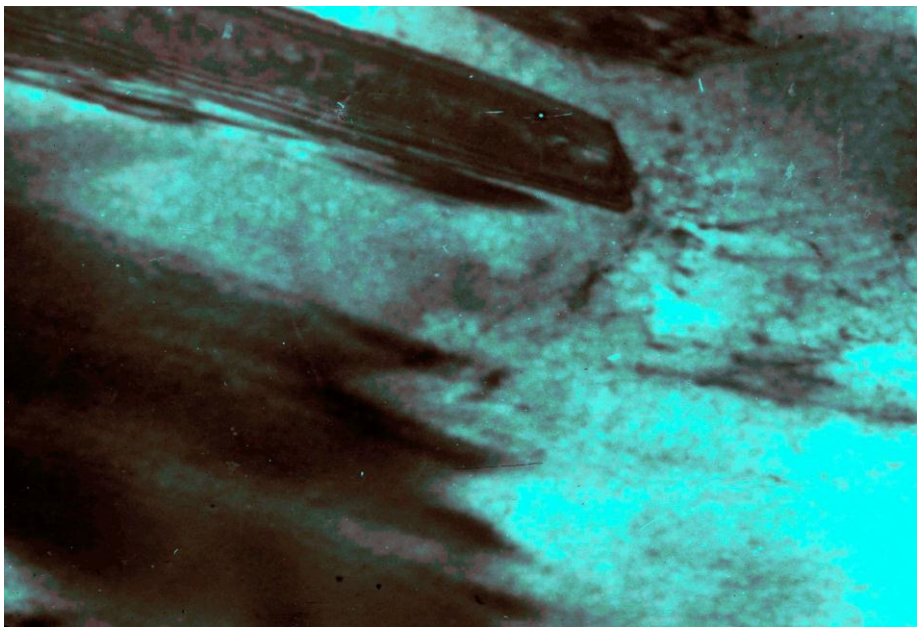

Fig 48, Deformation twins in indium as seen in the electron microscope. (Dasarathy [19, 20])

0.5 μm

Remaut et al [21] have also observed in the electron microscope significant mechanical twinning in foils of indium at -85^{0} C.

4.3. Grainboundary migration and other related phenomena in indium deformed at a sub-zero temperature.

Given below is a short extract of work that had already been published as well as exhibited [22-24].

Samples were deformed by ~30% at liquid nitrogen temperature (- 193 ^{0} C).Immediately after, the deformed samples were transferred to a 1 litre dewar containing liquid nitrogen. They were kept in the dewar until the liquid nitrogen had completely evaporated over a period of 24 hr. At the end of this stage, the sample temperature rose slowly to + 20 ^{0} C. The samples were prepared for metallographic studies. In between these studies, they were kept in a dessicator and aged at 20 ^{0} C for periods of up to 800 hours. The samples were examined at regular intervals during the ageing period. Fig 49 shows the fully recrystallised microstructure at the start of ageing.

1000μm

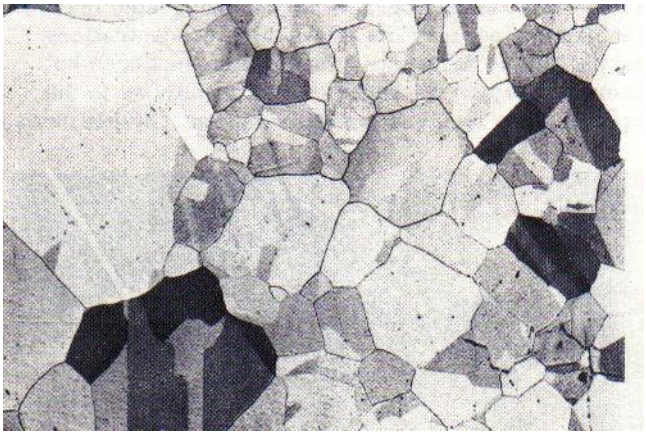

Fig 49 . Microstructure at the start of ageing at 20^{0}C

The grain size was mixed. Several annealing twins were also present. Selective etching was employed [24] to reveal the microstructure prior to recrystallisation. Figs 50 and 51 show examples where the prior boundaries are revealed by etch pits.

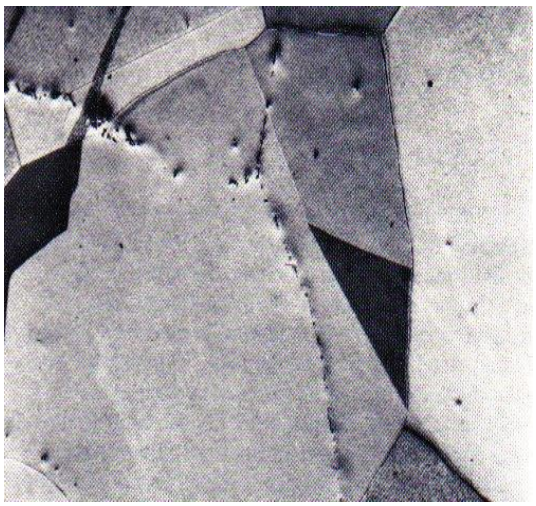

By far the most interesting developments occurred during ageing at 20^0 C. Grain boundary migration was soon evident and its course is shown in Figs 52 a-c.

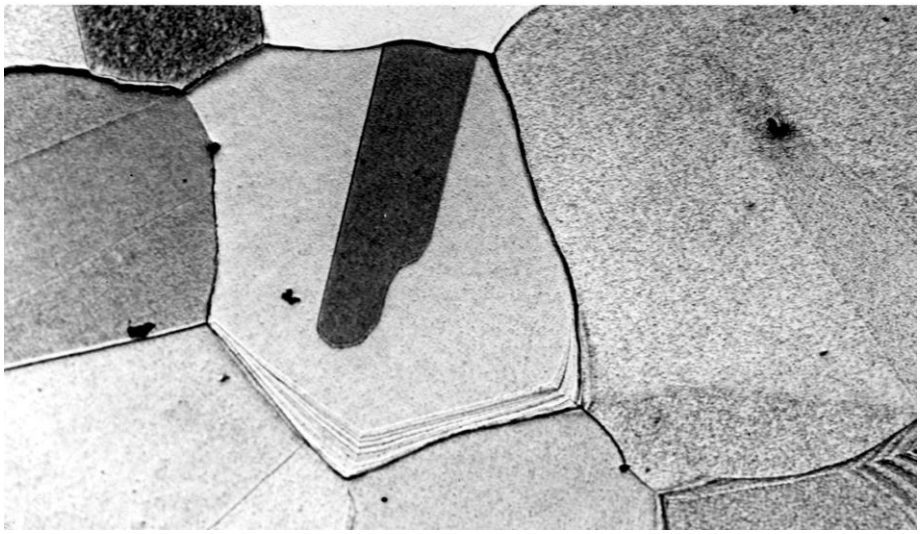

Fig52

a.260hr

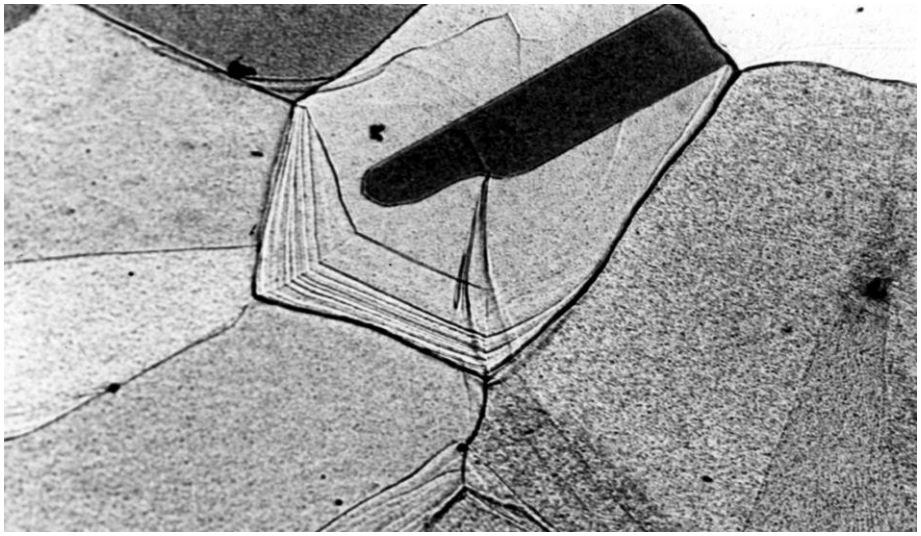

200μm

b.460hr

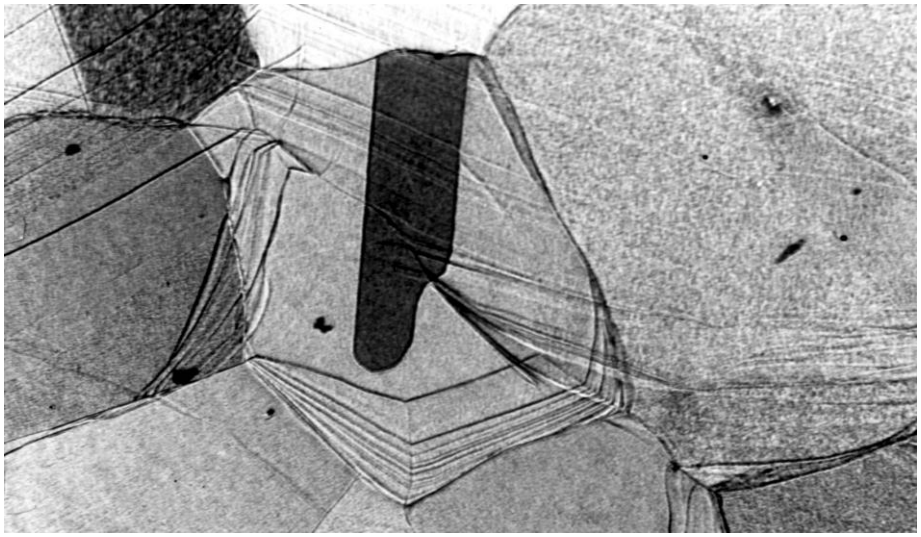

c.800hr

Indium melts at ~430 ^{0} K. Recrystallisation in most metals and alloys normally occurs at ~0.5 T melting point , ^{0}K. On this basis, in theory, the samples may have recrystallised at ~ 215 ^{0}K ie. ~ -60 ^{0} C ie. recrystallisation must hence have taken place between -193 ^{0} C and + 20 ^{0} C. It is clear from Fig 49 that recrystallisation had occurred by the time the samples reached 20 ^{0}C. The driving force for normal grain growth would have been insignificant at a temperature as low as 20 ^{0} C; the only process energetically feasible would be limited grain boundary migration. Indeed, this was what occured in most of the boundaries to varying extents.

The role of vacancies in grain boundary migration has been well documented [25-27] . Boundary mobility depends on, amongst other factors, the vacancy concentration at the boundaries. Mengelberg et al [28] have indicated that plastic deformation at low temperatures creates vacancies in high concentrations. They also add that these vacancies do not anneal out as rapidly as in the case of room temperature plastic deformation. On this basis, deformation at -193 ^{0} C may create high vacancy concentrations. Hence, even after recrystallisation,there could still be a surplus / excess of vacancies which may lead to boundary migration seen in Figs.52 &53.

Fig 53 ------- 50μm
The course of boundary migration seen here is evidently influenced by a line of obstacles such as dislocations, as revealed by the etch pits. Another interesting point to note in Fig52 is that the spacing between successive positions of the boundary increases with the ageing time (compare Figs 52 a to c).

Dislocations are regions of high energy; etchants hence attack them preferentially. Figs 54 &55 show examples of the dislocations within the annealing twins seen in the samples at various stages of ageing.

Fig 54

Fig 55 .

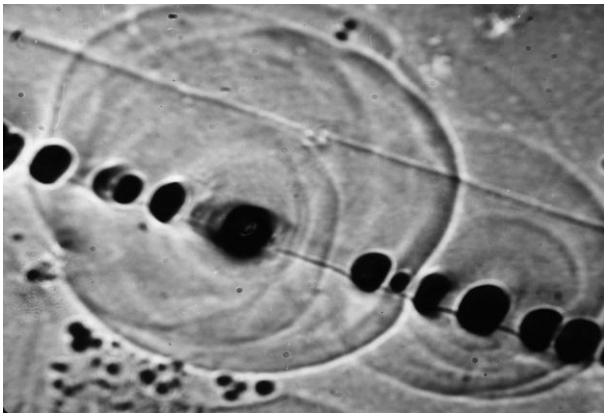

4.4 Is there a phase transformation in indium ?

Indium and tin are close neighbours in the Periodic Table. Some similarities in properties are to be expected. Indeed, there are .

1.Both the Fe-In and the Fe-Sn binary phase diagrams show regions of liquid immiscibility.
2.The tetragonal form of tin shows extensive twinning on deformation; the sound effect associated with this is known as 'the cry of tin'.
The tetragonal form of indium has been seen to twin extensively [19,20] .

The phase transformation from the cubic to the tetragonal form of tin is well known.However, what is not established as yet is whether a similar phase transformation exists in the case of indium. There are several pointers to suggest that there is indeed a phase transformation in indium. Experiments based on extrusion, compression, internal friction,tensile measurements, dilatometry, measurements of elastic constants and volume expansion coefficients as well as electron microscopy have strongly indicated a phase transformation at about 160-180 ^{0} K [20] . Whilst indium is tetragonal at room temperature, it may well have a different crystal structure below ~ 160-180 ^{0} K.

It is hoped that some readers of this document might be tempted to pursue this line of enquiry.

4.5 The deformation and recrystallisation behavoiur of bismuth

Bismuth is rhombohedral in crystal structure and melts at 544 ^{0} K. Its twinning behaviour is discussed by Smallman [15].

Samples of high purity bismuth were deformed by ~30 % in compression at liquid nitrogen temperature, -193 ^{0} C. Immediately after, they were brought up to room temperature and metallographically examined. Examples of the microstructures seen are given in Figs. 56&57.

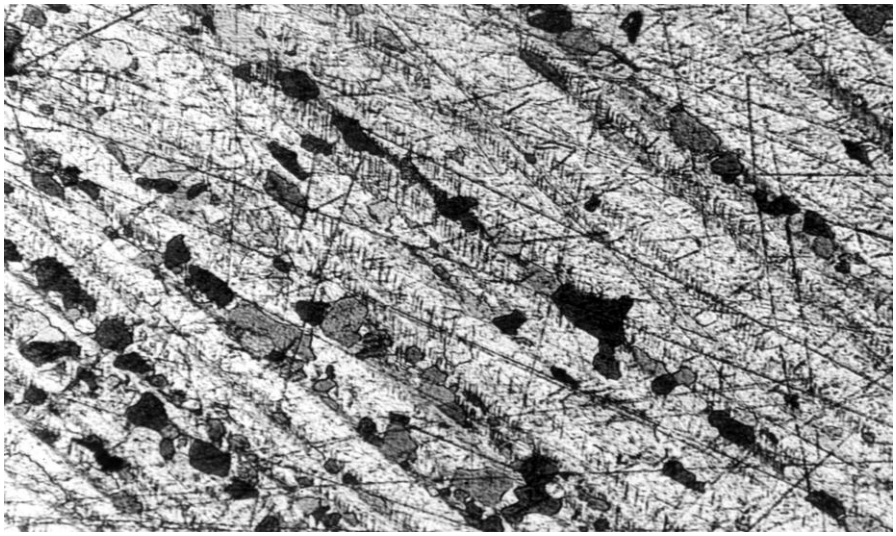

Fig 56

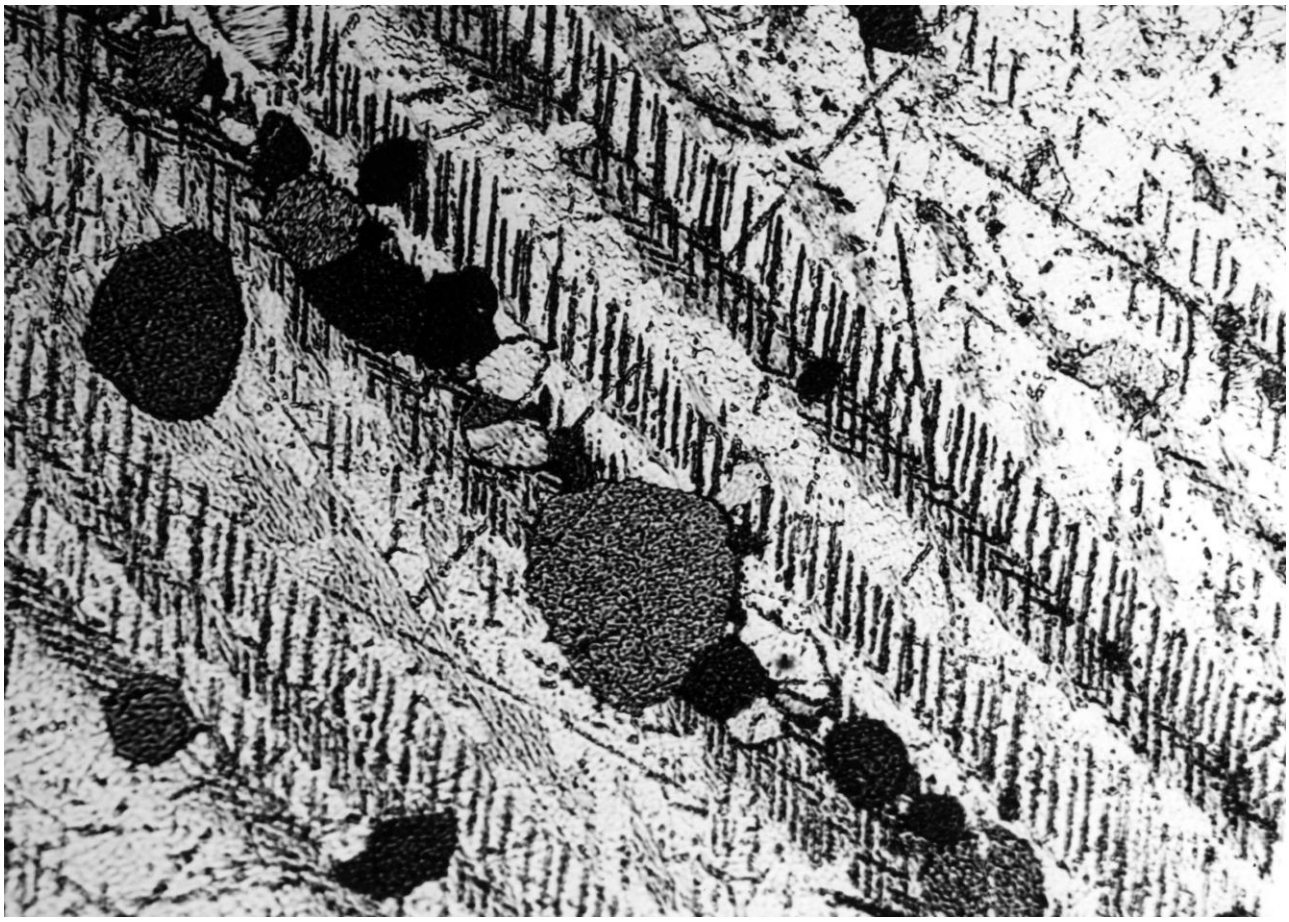

Fig 57 Same as in Fig 56 but at a higher magnification

When the criterion that most metals and alloys recrystallise at and above ~ 0.5 T melting point , in ^{0} K , is applied here, bismuth should recrystallise at ~272 ^{0}K. Evidently, this process is well under way at room temperature, as seen in the above figures. Parallel bands of deformation twins indicate that twinning has been the main mode of deformation. Nucleation of recrystallisation in the heavily twinned regions and the growth of the recrystallised grains are seen clearly in Fig 57.

4.6. Neumann bands in 3% silicon steels

The process of secondary recrystallisation in 3% Si steels has already been dicussed in Sec 3.6.3 page 24. Essentially , the microstructure consists of large ferrite grains. It is generally known that deformation at room temperature of ferrite occurs almost solely via slip. However, the presence of 3% Si favours, alongside slip, the formation of deformation twins, known as neumann bands [29]. These bands in pure iron have been known [15] to occur under conditions of explosive or impact loading.

Fig 58. Neumann bands in rolled 3% Si steels (after P.Moore [16])

These bands, seen in Fig 58, are made up of fine twin lamellae. It is interesting to note that although these bands normally appear either under low temperature deformation or under impact or shock loading, the presence of 3% silicon renders these rolled electrical steels to exhibit this behaviour.

4.7. Deformation, recrystallisation in Al and precipitation hardening in Al-Cu alloys

The preceding examples have considered cases where the levels of deformation prior to recrystallisation have increased gradually . The case under study here deals with aluminium of commercial purity cold rolled by ~60% and annealed to produce a fully recrystallised structure [30].

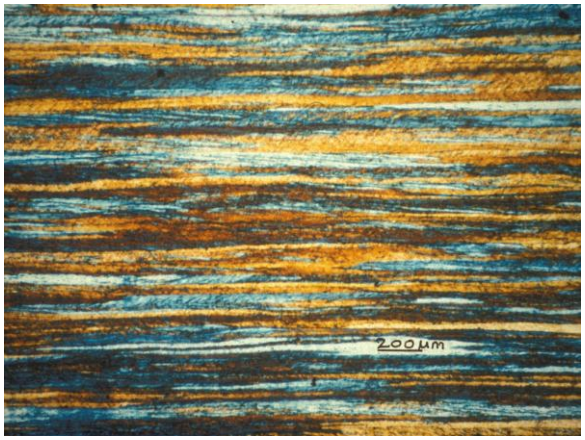

.

Fig 59 after cold rolling

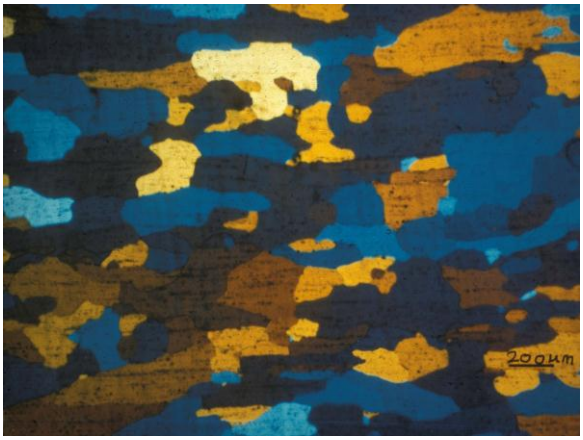

Fig 60 after annealing

Selective etching was employed to reveal the crystallographic orientations of the grains.The different colours indicate different orientations. Fig 59 shows the grains to be elongated in the rolling direction. It is to be noted in Fig 60 that the colours are randomly distributed; this suggests that the annealed sheet does not exhibit a strong preferred orientation; this is also described as a random texture. It is also interesting to note the absence of annealing twins in Fig 60.

The absence of a strong preferred orientation in the silicon steel after recrystallisation was considered in Fig 38, sec 3.6.3. The magnetic domain boundaries were aligned in different directions in the grains. Essentially, the texture, at this stage of the process, was random.

These examples show that several etching techniques are available to reveal microstructural details such as those in duplex stainless steels (Fig 43), prior boundaries and dislocations via etch pits (Figs 50, 51, 53-55) as well as to show whether a given microstructure is highly crystallographically oriented or not via selective etching to reveal the magnetic domain boundaries (Fig 38) or the colour distributions amongst the recrystallised grains (Figs 59,60).

Effects associated with precipitates have been covered in earlier sections . These included issues in steels such as precipitation:- during hot rolling (sec 3.5) , concurrent with recrystallisation on batch annealing (sec3.6.3) , the role of precipitates in secondary recrystallisation (sec 3.6.4) as well as carbon precipitation on dislocations in bake hardening steels (sec3.6.5).

The Al-Cu system is an excellent example to consider another interesting aspect, precipitation hardening. Considering the Al rich end of the Al-Cu binary phase diagram[2]

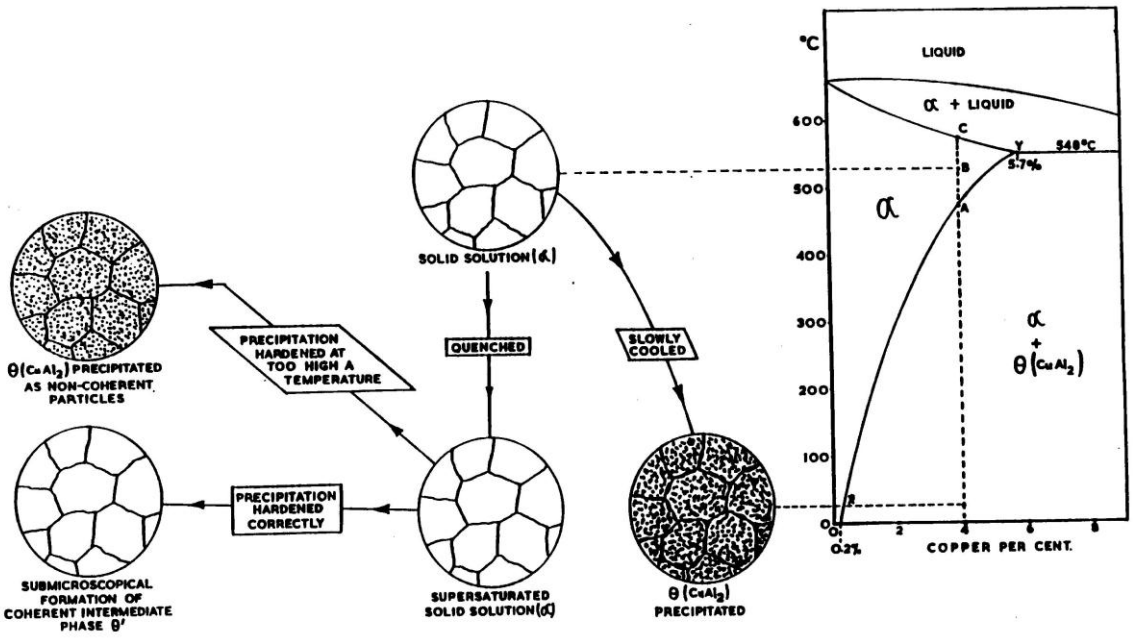

Aluminium-rich End of the Aluminium–Copper Equilibrium Diagram, Showing the Observed Microstructural Effects of Slow Cooling and Precipitation-hardening.

Fig 61 (source unknown), an alloy with 4%Cu may be quenched from >540 ^{0} C to room temperature to give the single phase ,α,which contains Cu in a supersaturated state .Given an appropriate heat treatment, θ , the equilibrium precipitate, $CuAl_2$,will form. However, this is a multi-stage process. On ageing at < 180 ^{0} C, copper-rich zones that are coherent with the lattice will form first. Guinier and Preston [32] were the first to detect this stage by low angle x-ray scattering. These are known as GP_1 and GP_2 zones. These metastable precipitates, θ'', θ' form prior to the precipitation of the equilibrium precipitate, θ ie $Cu Al_2$.

The following examples , taken from the work of George Vander Voort [35], show the microstructures of an Al-4% Cu alloy quenched and aged at temperatures >180^{0}C. These examples do not show the **metastable** preciptates since the techniques involved neither x-ray low angle scattering nor transmission electron microscopy. However, what the examples do show is the clear evidence of the **stable equilibrium** precipitates, $CuAl_2$.

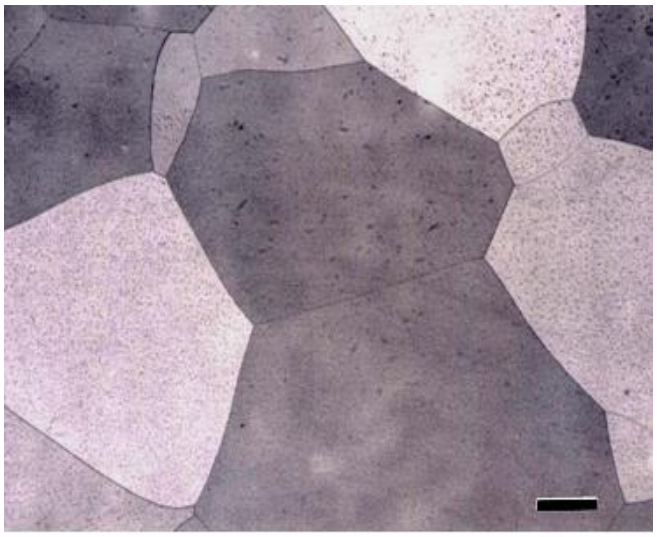

Equiaxed alpha grain structure in solution annealed (552 °C, 1025 °F for 1 h, water quench) Al – 4 % Cu etched with Keller's reagent. Magnification bar is 200 µm long.

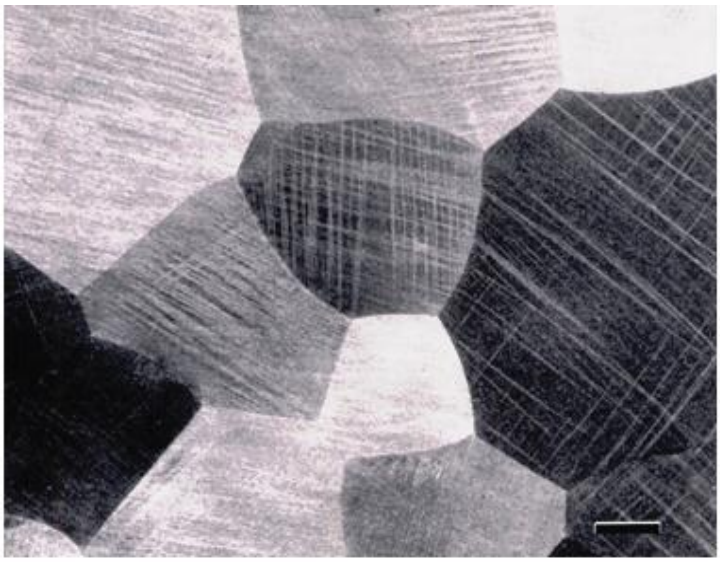

ed alpha grain structure with criss-cross marks in solution annealed and aged (552 °C, 1025 °F for 1 h, wate r, 260 °C, 500 °F – 1 h, air cool) Al – 4 % Cu etched with Keller's reagent. Bar is 200 µm. Markings a reduc to ecipitation in the alpha phase.

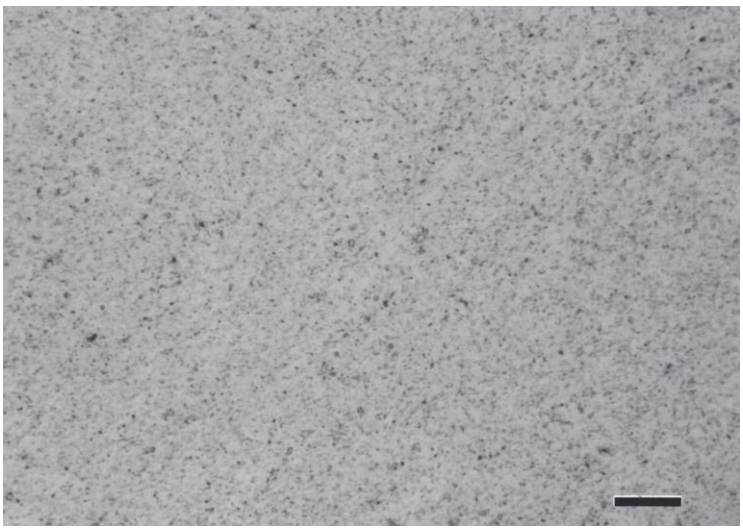

Very fine precipitates in solution annealed and aged (552 °C, 1025 °F for 1 h, water quench, 260 °C, 500 °F – 1 h, air cool) Al – 4 % Cu etched with aqueous 0.5% HF. Magnification bar is 10 µm long.

Top left Fig 62/ solution treated at 550 ^{0} C for 1hr/ water quenched/scale 200µm/ α **phase**/Keller's reagent etch
Top right Fig 63/
Same sample aged at **260** ^{0} C/1hr/scale200 µm/ **fine pptn. causes markings on the α phase/** Keller's reagent etch

Bottom left Fig 63a/same as in Fig 63 but 0.5% aq Hf etch/ **very fine pptes**/scale 10 µm

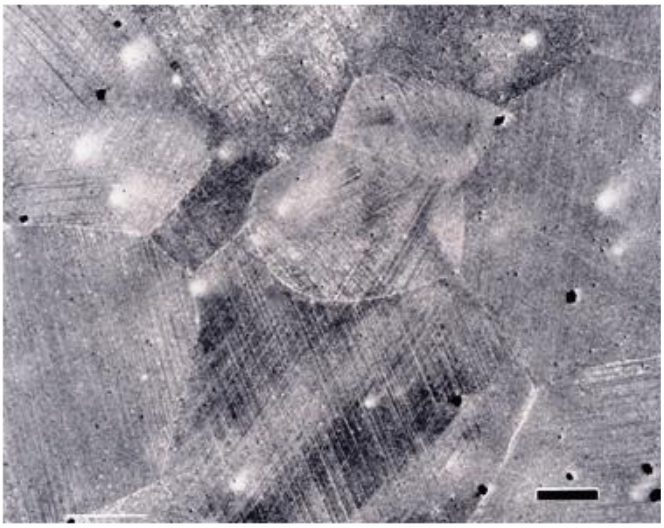

Equiaxed alpha grain structure with criss-cross marks in solution annealed and aged (552 °C, 1025 °F for 1 h, v quench, 316 °C, 600 °F – 1 h, air cool) Al – 4 % Cu etched with Keller's reagent. Bar is 200 µm. Markings a redu fine precipitation in the alpha phase.

Fig 64 aged at **316 ^{0} C**/1hr/scale 200µm markings are due to fine pptn in the α phase

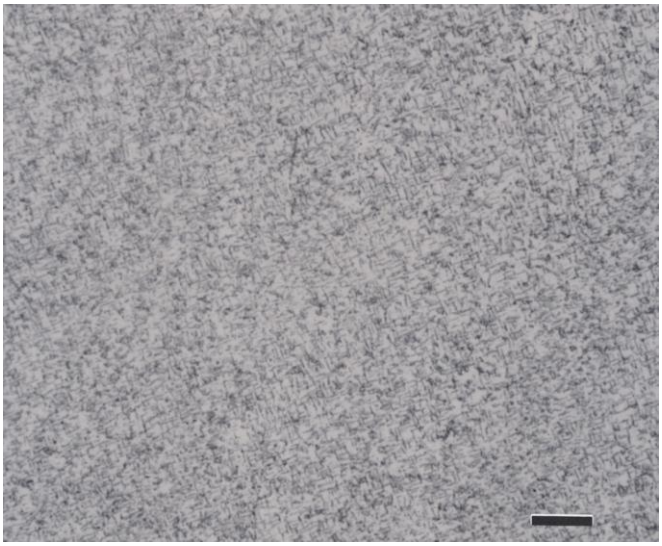

Fine precipitates in solution annealed and aged (552 °C, 1025 °F for 1 h, water quench, 316 °C, 600 °F – 1 h, air cool) Al – 4 % Cu etched with aqueous 0.5% HF. Magnification bar is 10 µm long.

Fig 64a same sample as in Fig 64/very fine pptn/scale10µm/ same etch as in Fig 63a

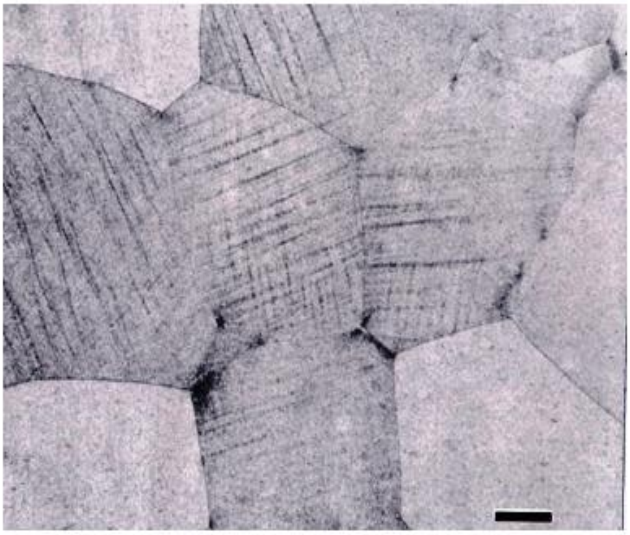

Equiaxed alpha grain structure with criss-cross marks in solution annealed and aged (552 °C, 1025 °F for 1 h, water quench, 371 °C, 700 °F – 1 h, air cool) Al – 4 % Cu etched with Keller's reagent. Bar is 200 µm. Markings a re due to fine precipitation in the alpha phase.

Fig 65 aged at **371 ^{0} C**/1 hr/scale 200µm/ pptn markings on the α grains /Keller's etch

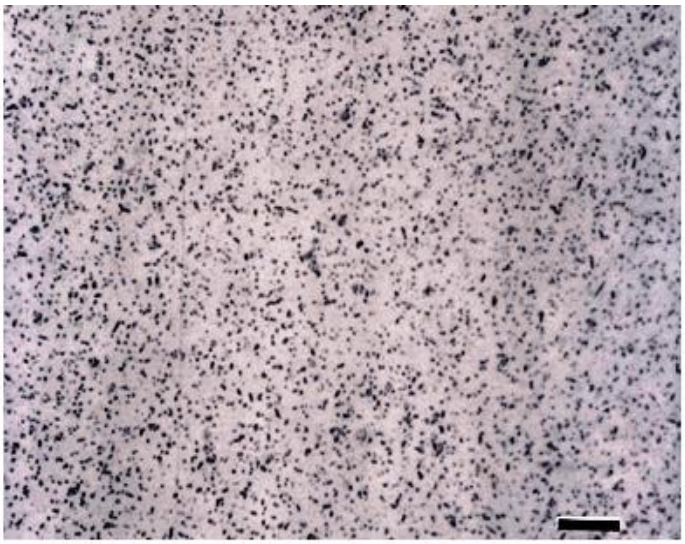

Very fine precipitates in solution annealed and aged (552 °C, 1025 °F for 1 h, water quench, 371 °C, 700 °F – 1 h air cool) Al – 4 % Cu etched with aqueous 0.5% HF. Magnification bar is 10 µm long.

Fig 65a same as Fig 65 fine pptn/ scale10µm/same etch as in Fig 63a

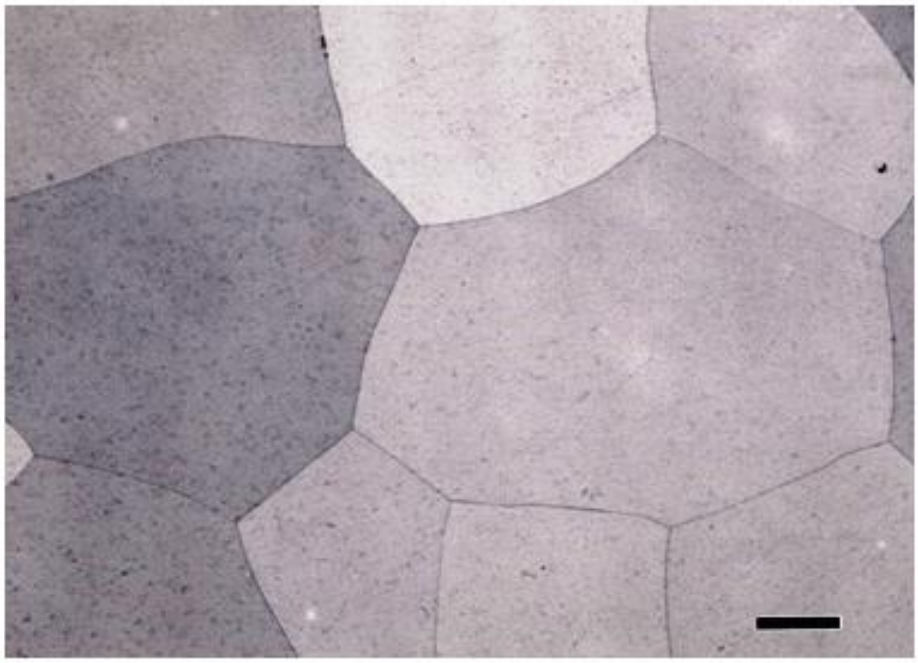

Equiaxed alpha grain structure in solution annealed and aged (552 °C, 1025 °F for 1 h, water quench, 538 °C, 1000 °F – 1 h, air cool) Al – 4 % Cu etched with Keller's reagent. Magnification bar is 200 μm long. Criss-cross markings are no longer present because the high aging temperature has dissolved nearly all of the fine precipitates in the alpha phase. Compare with the solution annealed image at the same magnification.

Fig 66 /aged at **538 ^{0} C**/1hr/ no markings on the α grains,high ageing temp. causes almost all the pptes. to go back into solution within the α phase / scale 200μm.

These observations form the basis of the 'age hardening' series of alloys. Essentially, these

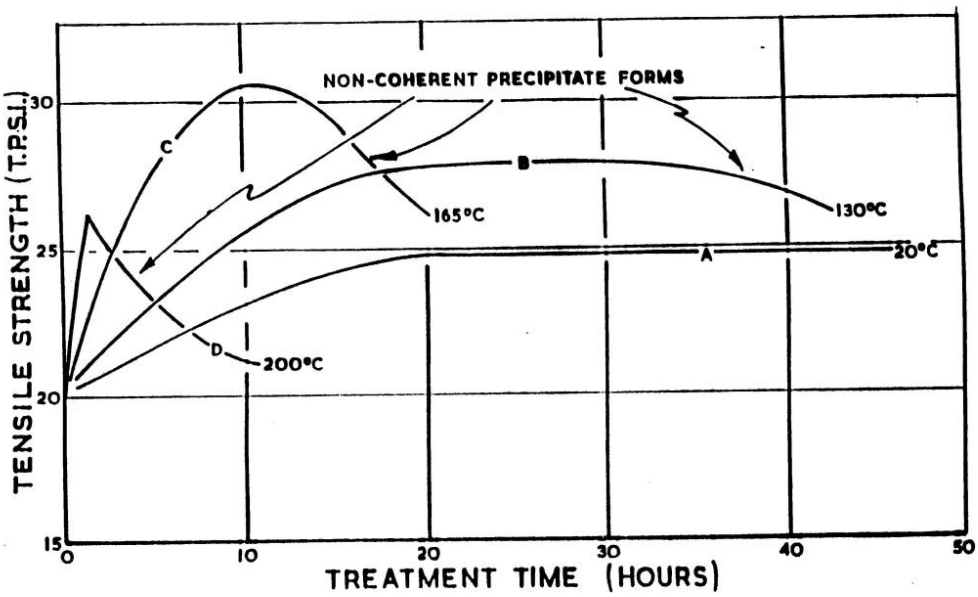

The Effects of Time and Temperature of Precipitation-treatment on the Structure and Tensile Strength of a Suitable Alloy.

Fig 67 (source unknown)

are Al-alloys with additions of elements,Ag, Mg-Si,Mg-Cu and Mg-Zn to manipulate microstructures and, hence, the properties [15]. The 'Duralumin' series of alloys belongs to this group. In the case of Al-Cu alloys, quenching from > ~ 550 ^{0} C and ageing at an optimum temperature for an optimum time leads to a very fine sub-microscopic dispersion of the θ'' and θ' precipitates that are coherent with the matrix . The coherency strains associated with these precipitates contribute to the significant increase in strength. When this stage is passed , for example, by ageing at higher temperatures, as seen in the above examples, the incoherent,equilibrium precipitate, $CuAl_2$ forms, coherency strains disappear and this leads to 'over-ageing' and, hence, a significant drop in strength Fig 67.

Indeed, this is the basis of the normal heat treatment cycles used in age hardening Al alloys.

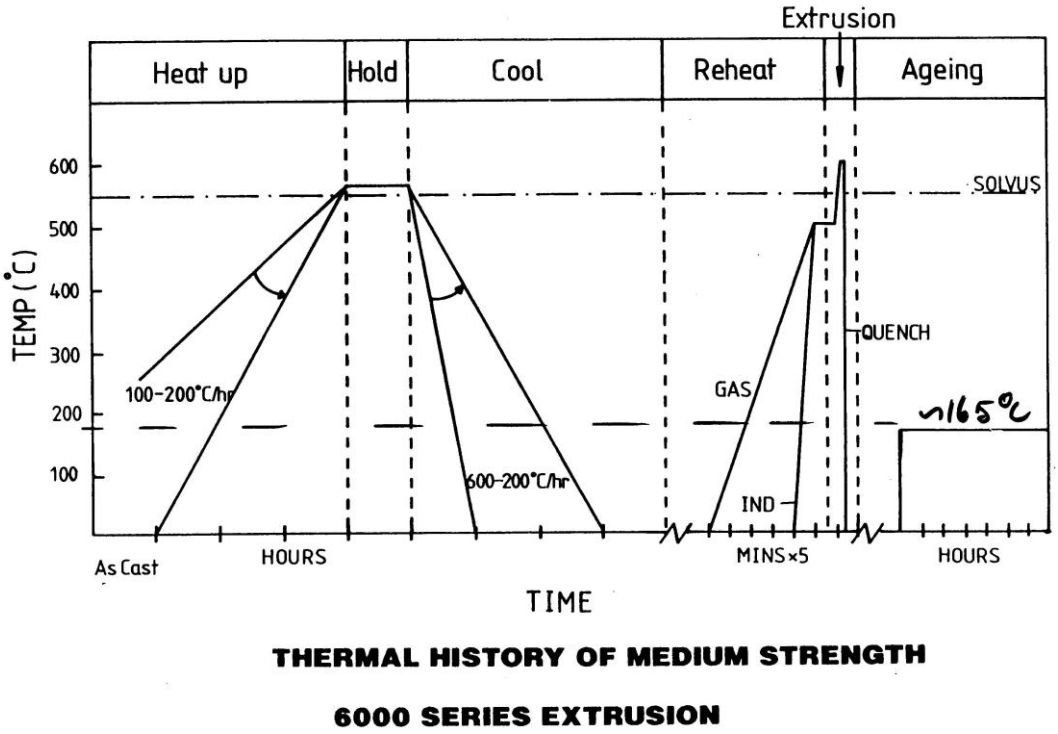

Fig 68 (source unknown)

Fig 68 is an example of a cycle applied to Al extrusions. Starting from the left of the diagram, we note that the as –cast bars or billets are heated to ~550 ^{0} C and soaked for a short time; this is designed to eliminate the as-cast dendritic grain structure as well as to eliminate traces of segregation, essentailly, this is a homogenisation anneal.. The material is then rapidly cooled down to room temperature. Now follows rapid heating with gas or by induction to ~ 600 ^{0} C ; the material is extruded at this temperature into the desired sections and sizes.The sections are now quenched back down to room temperature. Finally, the quenced sections are aged at ~165 ^{0} C for ~7 hours for maximum precipitation hardening.

4.8 Copper, brasses and bronzes

Austenitic stainless steel (Fig 42), aluminium (Figs59,60) and some of its alloys as well as copper and some of its alloys have one thing in common; they belong to the FCC group. As such, they have a mutiplicity of slip systems, deformation at room temperature occurs via slip and they are very ductile.

OFHC (oxygen free high conductivity) copper is widely used in electrical applications, an example of which is given in Fig 69. Fig 70 shows the microstructure of pure copper, (OFHC) grade.

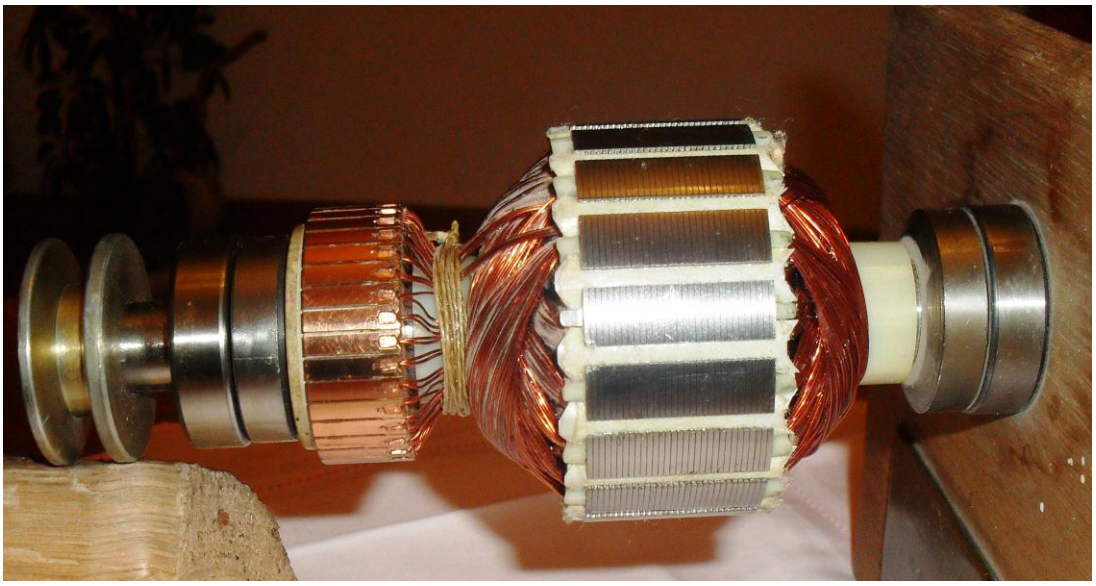

Fig 69 . Motor assembly (after Ewald Holzem [36])

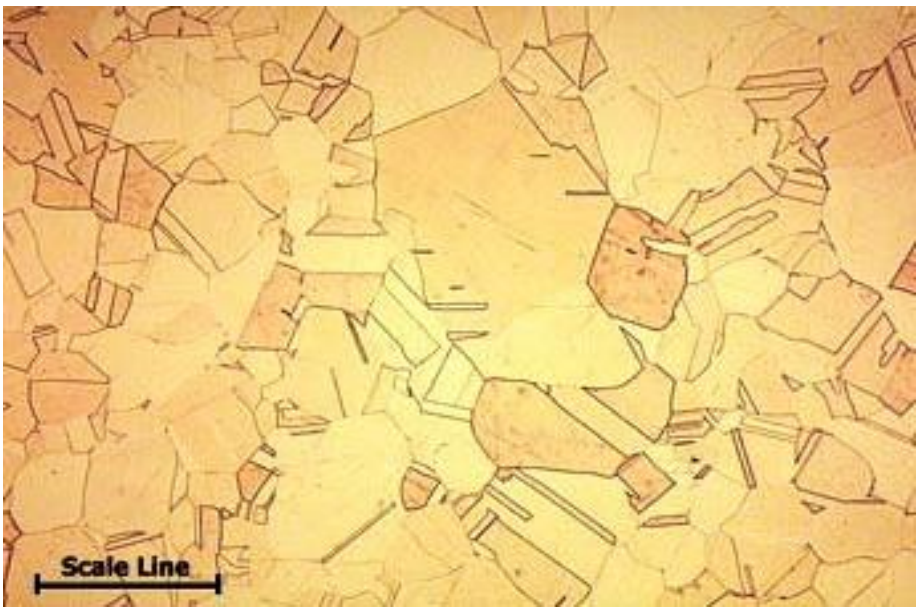

Fig 70
Scale bar=125μm

OFHC copper was rolled into rods, these were then annealed at a high enough temperature for recrystallisation and grain growth to occur. Numerous annealing twins of varying widths can be seen. Annealing twins grow in width during grainboundary migration that occurs during the later stages of annealing.

Brasses are essentially alloys of copper with zinc. They retain many of the properties inherited from copper. Microstructurally, Fig 71, they are similar to copper when recrystallisation and significant grain growth have taken place during annealing at an appropriate temperature for a long enough time.

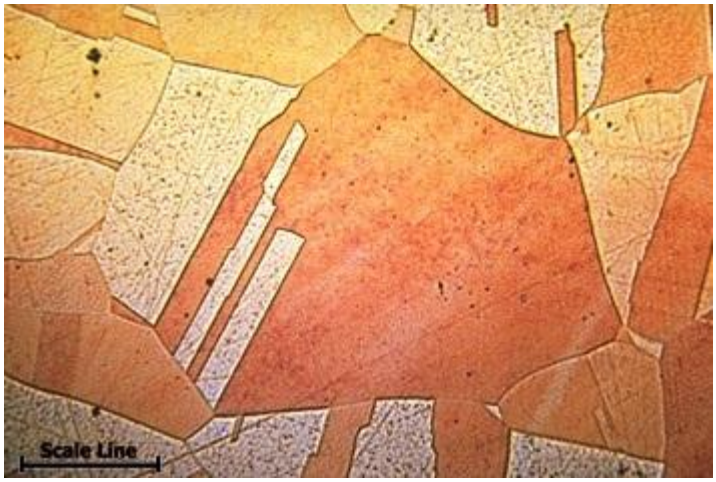

Fig 71
Scale bar=25μm

Fig 71 shows the microstructure of an alloy with ~97% Cu & ~3% Zn with traces of Fe &Pb

A very good example of brasses is the cartridge brass made up of ~70% Cu &~30%Zn. Cold rolling leads to the appearence of slip lines; deformation takes place by slip, Fig 72a-d. (reproduced with the permission of George Vander Voort [35])

Fig 72a cold rolled by 30%

Fig 72b cold rolled by 40%

Fig 72 c cold rolled by 50% Fig 72 d cold rolled by 60%

(Figs a-d scale bar length= 100μm)

The above figures clearly show that deformation occurs via slip and that the density of the slip bands increases with the level of deformation. It is interesting to note that whilst slip is the dominant mode in FCC materials, twinning becomes the dominant mode in indium (tetragonal)/(Fig48) as well as in bismuth (rhombohedral)/ (Figs 56 &57) .

Hot or cold working followed by annealing results in a recrystallised structure as shown in Fig 73.Cartridge brass is well known for its excellent formability; mass produced deep drawn components such as all forms , sizes and shapes of bullets, cartridges and other types of ammunition are deep drawn from the sheet over the stages 1-3, Fig 74. Depending upon the severity of the draw, components are often given an intermediate softening anneal prior to the final stages of deep drawing. The deep drawability of brasses, in general, is known to be superior to that of aluminium and its alloys.

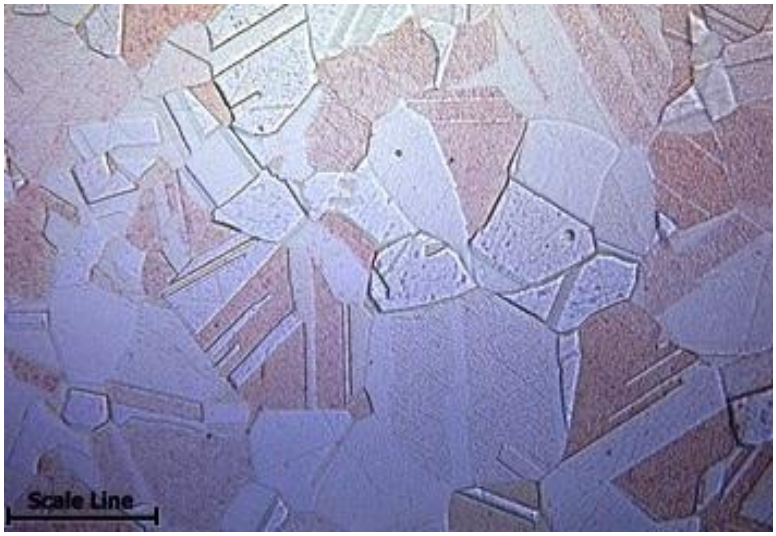

Fig 73
Scale bar=25μm

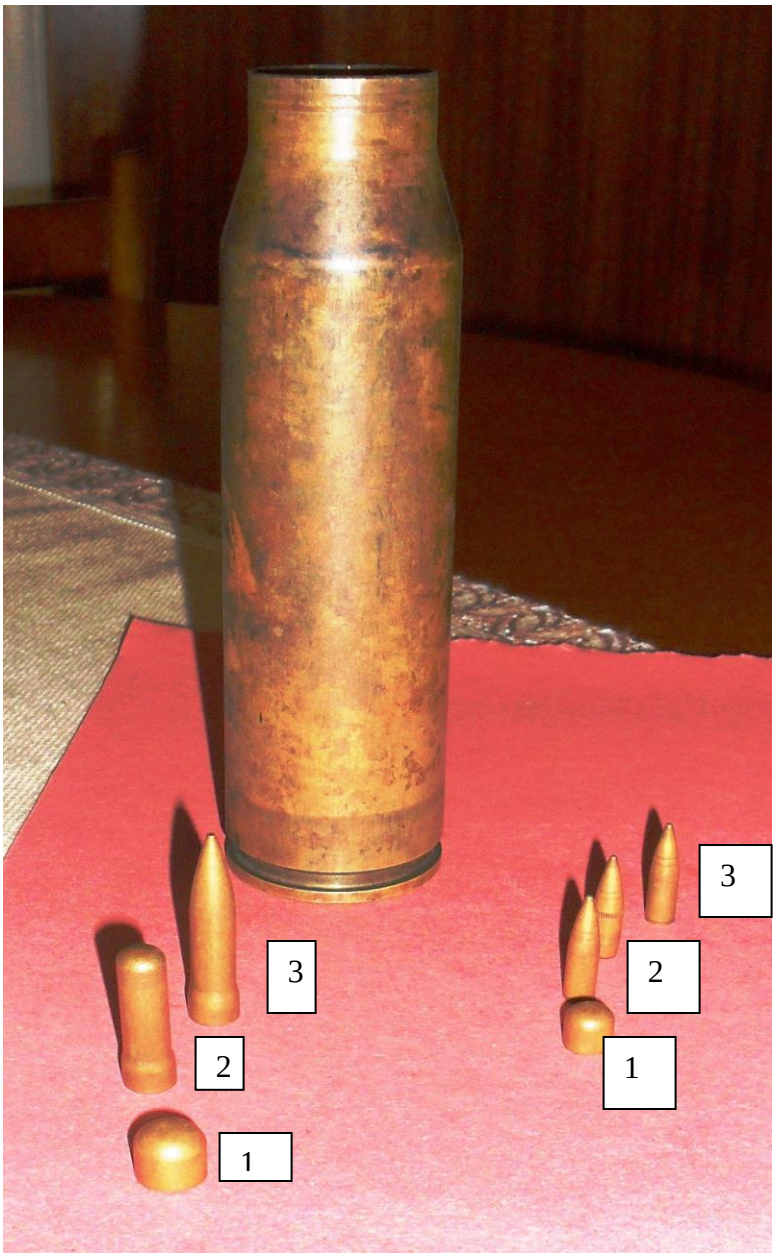

Fig 74

Examples of bullets and cartridges produced by deep drawing from rolled and annealed cartridge brass sheet of appropriate thicknesses

The bullets shown in Fig 74 are of two different sizes and are deep drawn over the stages 1 to 3.

Copper alloyed with tin produces bronzes. A good example is the phosphor bronze that contains about 3-10% Sn and upto ~ 1.0 % P besides traces of Zn, Fe and Pb. Common to most alloys of copper, these show similar microstructures on annealing(Fig 75).

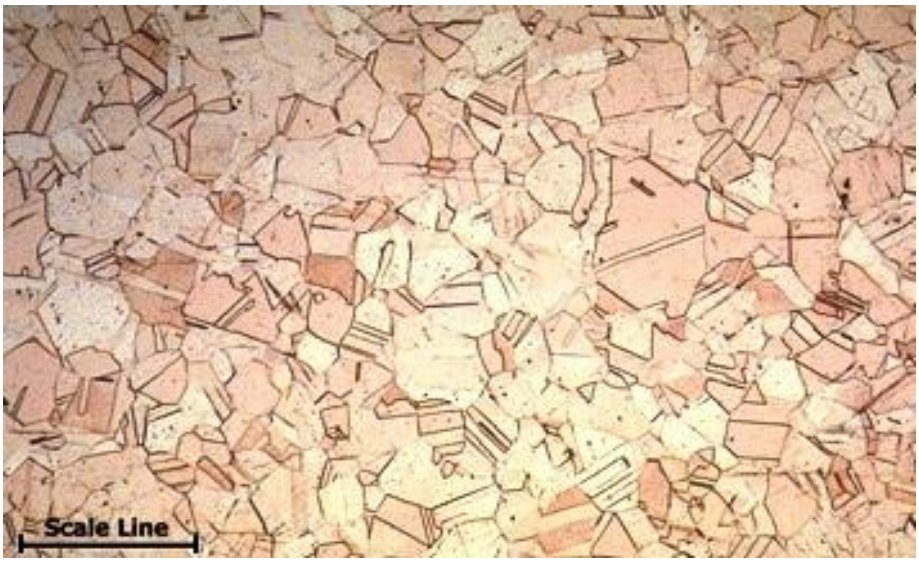

Fig 75
Scale
bar=125μm

Noted for their good properties such as toughness, fine grain size and hence, superior strength, low coefficient of friction and resistance to fatigue , phosphor bronzes are used in applications such as springs, bolts, parts for cryogenic use, brass musical instruments,etc.

Microstructures of copper, brasses and bronzes are from the Copper Development Association [37].

5. Superplastic materials

As far back as in the 1930's, Pearson [32]was amongst the first, if not the first, to record superplastic behaviour in metallic materials; he noted this in a Bi-Sn eutectic alloy, deformed at a high enough temperature and at a slow strain rate. The concept was later developed in the 70's and the 80's , especially by the aerospace industry.Today, it is a well accepted and adopted practice in many sections of the industry [1].

Essentially, this is deforming a material with a very fine grain size at a high enough temperature and at a slow enough strain rate so as to avoid workhardening. Grainboundary sliding is one of the theories put forward to explain superplasticity.Ideally, total elongations in excess of ~400% can be achieved. Compare this figure with a total elongation of ~40 % in some of the most ductile sheet steels covered in the earlier sections.

One of the basic requirements is that the starting material is to have a very fine grain size; examples of some Ni-based , Al –based and Ti- based superplastic materials are given in Figs 76-78.

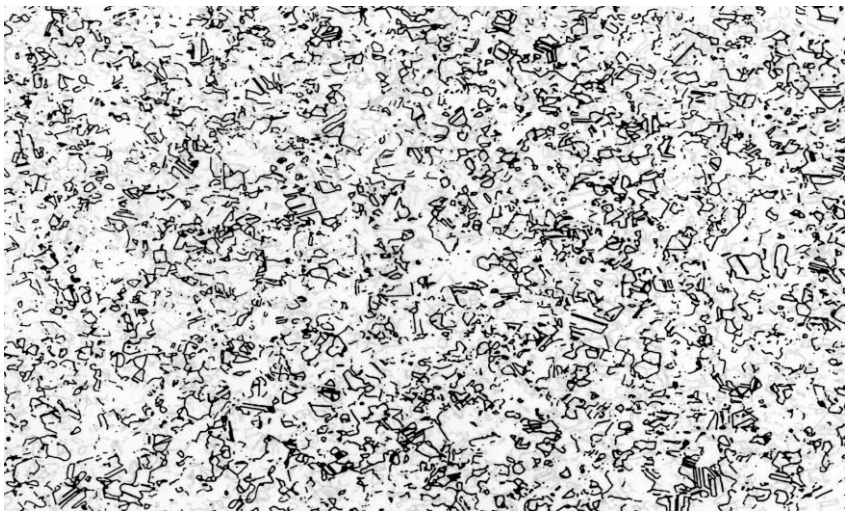

Fig 76 Ni-based
(source unknown)

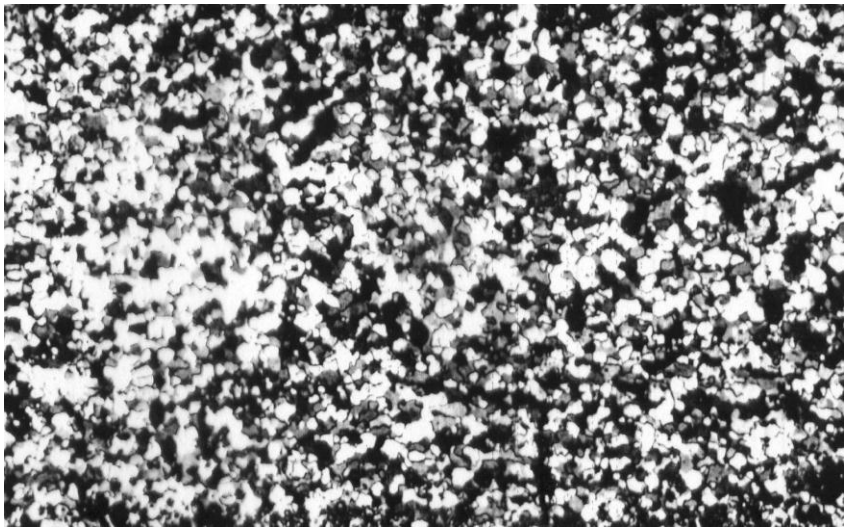

Fig 77
Al-based alloy
8000 series alloy
ALCAN labs.
(Private commun)

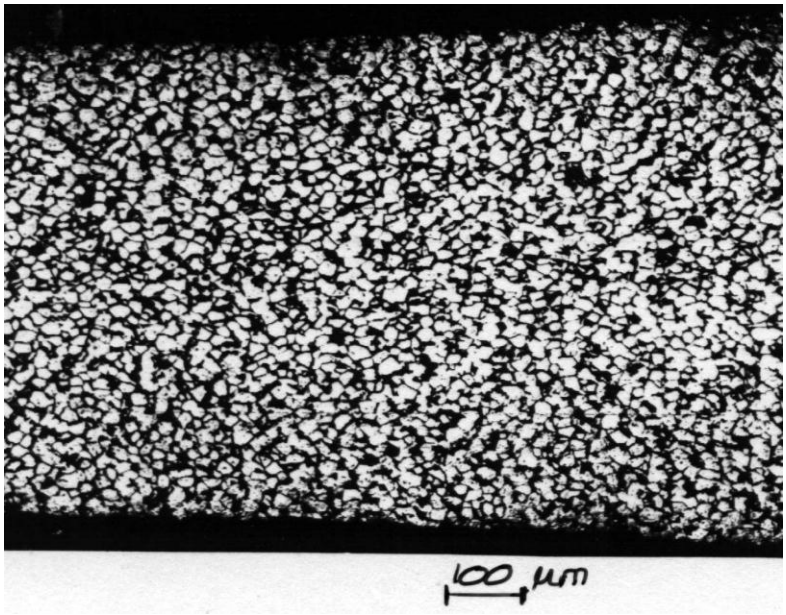

Fig 78
Ti alloy
(private communication from Sylvia Williams, Brit.Aero Space/ Airbus Ltd, July 1993)

An examination of Figs 76-78 shows that the materials have been processed so as to produce a very fine grain size.

Pearson's work showed superplastic behaviour in a Bi-Sn eutectic alloy. Several similarities between tin and indium have been outlined in sec 4.4, P 36 of this report. If a Bi-Sn eutectic alloy showed superplastic behaviour, the question arose as to whether a Bi-In eutectic alloy would also show the same.

High purity Bi and In were used to prepare the eutectic alloy of 66 wt% In and 34 wt%Bi. The eutectic temperature was 72^{0} C [33] . The as-cast alloy showed a fine eutectic structure. Fig 79a. As- cast specimens were rolled by ~85% to sheet samples O.036 inches thick at 20^{0} C . Tensile specimens (250mm gauge length &130mm wide) were prepared.Rolling changed the microstructure to that seen in Fig 79b. Specimens were tested at different strain rates . The best elongation obtained was ~450%. [34].

Fig 79a

30μm

Fig 79b

20μm

Electron microscope examination of the sample with the best elongation (~450%) showed microstructures similar to that given in Fig 80.

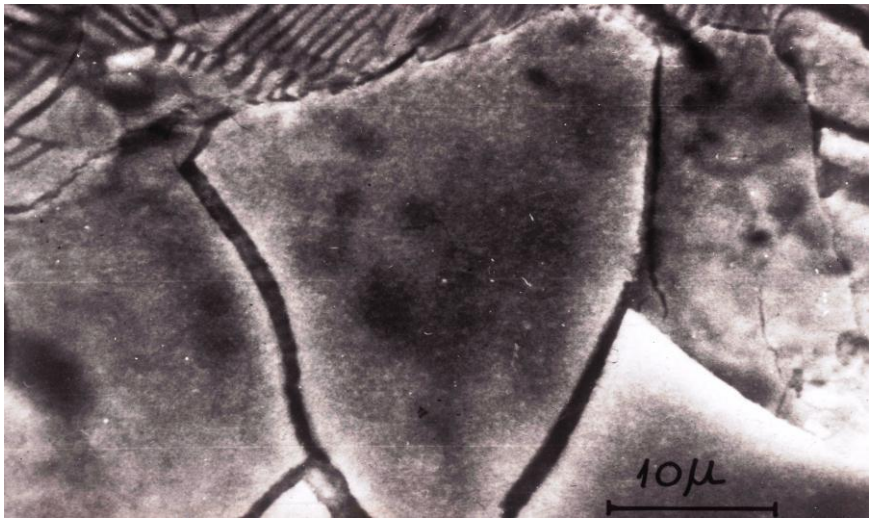

Fig 80.Microstructure close to the fractured end of the test piece [34]

Whilst the lamellar network of the eutectic regions could be seen in the background, the grains seen in the foreground may provide some evidence of or , perhaps, suggest grainboundary sliding [34].

6. **Concluding remarks and acknowlegements**

It is hoped that the present compilation of microstructures in a range of materials will be of benefit to students, researchers as well as members of academic staff dealing with metallurgy and materials sciences. The contents could also prove to be useful to those employed in the sheet steel industry.

If read in conjunction with the earlier compilation 'Examples of fractures, failures and rejections in engineering materials and components' [1] , a better understanding could be achieved of the issues such as
Why do materials fail?
What is the role of the microstructure ?
What can be done to avoid the incidence of failures by generating an appropriate microstructure compatible with the properties required in the material as well as in the components derived from this material.

In producing this document, I have been helped with the information provided by several friends and former colleagues. I place on record my thanks and gratitude to
A.Dunn, R.Evans, D.T.Gawne, E.Holzem, L.K.Lyons, P.Moore, A.Murray, P.Oldroyd, P.Richards, P.Swanson, G.Vander Voort, P.Webster (Copper Development Association) and S.Williams.

C.Dasarathy February 2012

7. References

1. C.Dasarathy,'' Examples of fractures, failures and rejections of engineering materials and components''; the document is available as a pdf file at Wikimedia Commons; this is listed as
' **A book on failures' by Cuppam**/ Ticket Number #2011082310006175/ 25th of August 2011. This can accessed at Wiki/File. Book on failures. PDF and at http://en.wikiversity.org. ; it is to be found in the 'Materials Sciences' section of the website.
2.M.Hansen & K.Anderko, Constitution of Binary Alloys, 2nd Ed. Mcgraw-Hill, New York, 1958
3. Philip Oldroyd, private communication

4.R.W. Russel Evans, Univ. of Wales, Swansea, private communication
5.Paul Richards, private communication
6.J.J.Witts, T.A.Kop, Y.Van Leeunen,J.Seitsma & S.Van Der Zwaag, Mat.Sci & Eng.A.283, 234-241,May 2000
7.E.O.Hall, Proc.Phys.Soc. 64B,747,1951
8.N.J.Petch, JISI,25,174,1953
9.R.W.Russel Evans, Univ. of Wales, Swansea, private communication
10.C.Dasarathy & R.C. Hudd, Z.Metallk. 60, 853, 1969
11. Adrian Dunn, Ph.D Thesis, Univ. Liverpool, 1970
12. D.T.Gawne , private communication,1970
13. W.Jolley , JISI,205,321,1967
14.C.Dasarathy & R.C.Hudd, Acta Met, 15,1665,1967
15. R.Smallman, Modern Physical Metallurgy, London, Butterworths, 1962
16. Peter Moore, private communication
17.C.Dasarathy, Z.Metallk. 58,279,1967, Z.Metallk, 63,209,1972
18. C.Dasarathy, Trans.Met.Soc.AIME,245,1838, 1969
19.C.Dasarathy, Phil.Mag. 23,no.185,1235,1971
20.C.Dasarathy, Nature, 238,August28,141,1972
21. G.Remaut,A.Lagasse,S. Amelinckx, Phys. Stat. Solidi,6,723,1964
22.C.Dasarathy,Met.Soc.1,1784,1970
23.C.Dasarathy,ASM. Intl. Metallographic Exhibition, Hon.Mention,1972
24.C.Dasarathy, Praktische Metallographie,7,281,1970
25.K.T.Aust & J.W.Rutter,'Recovery & Recrystallisation of Metals',Interscience Publishers, New York & London, P131,1963
26.P.Gordon & R.A.Vandermeer,' Recrystallisation, Grain Growth & Textures, P205, American Society for Metals, Ohio, 1966
27.K.Lucke & H.P.Stuwe, 'Recovery & Recrystallisation of Metals,as in Ref 25, P171
28.H.D.Mengelberg,M.Meixner & K.Lucke,Acta Met,13,835,1965
29. G.M.Lusakov,A.A.Redikultsev& M.L.Lobanov, Met & Mat. Trans.39A,2278,2008
30 Aidan Murray, private communication.
31. P.Archer,private communication
32. C.E.Pearson J.Inst.Metals,54,111,1934
33. as in Ref.2, p313
34.C.Dasarathy,Z.Metallk.62,612,1971
35. George Vander Voort private communication, 2012
36. M.E.Holzem, private communication, 2012
37. Copper Development Association Archives ,2012